REALTIDE

Grant Agreement No 727689

Document Title:
Methodology for the fatigue assessment of composite material blades

Document No:
RLT-WP1-4-PDL-001-00

Status Code	Description
A	Accepted
B	Issued for Acceptance
C	Issued for Review
D	Information Only Approval not required
E	Cancelled

01	B	Comments from partners incorporated.	Joseph Praful Tomy	All Partners	Stephane Paboeuf
00	C	/	Joseph Praful Tomy Mael Arhant	Luc Mouton Peter Davies	Stephane Paboeuf
Rev No	Status	Revision Description	Prepared By / Date	Reviewed By / Date	Approved By / Date

European Commission
H2020 Programme for Research & Innovation

Advanced monitoring, simulation and control of tidal devices in unsteady, highly turbulent realistic tide environments

REALTIDE

Grant Agreement number: 727689

Project Acronym: RealTide

Project Title: Advanced monitoring, simulation and control of tidal devices in unsteady, highly turbulent realistic tide environments

Deliverable D1.4
Methodology for the fatigue assessment of composite material blades

WP 1
Increased Reliability of Tidal Rotors

WP Leader:
Bureau Veritas Marine & Offshore

Dissemination level:
Public

Summary:
A methodology for the evaluation of fatigue life of tidal turbine blades and loading test for composite materials in sea water that can be integrated in existing guidelines for designers.

Objectives:
Methodology to evaluate the fatigue life of tidal turbine blades.

Table of Contents

List of Figures

List of Tables

1 INTRODUCTION

Within Work package 1 of the RealTide project, the reliability aspect of tidal turbines is explored. The aim of this work package is to identify and characterize potential reliability issues for tidal turbines based on literature and partners experience in laboratory, in tank and at sea. Task 1.4 addresses the issue of reliability by identifying existing gaps in the fatigue assessment procedure for composite blades. The task aims to bridge this gap by developing a methodology for the evaluation of fatigue life of tidal turbine blades and loading test for composite materials in sea water that can be integrated in existing guidelines for designers. A literature review is performed to identify the state-of-the-art approaches in modelling fatigue behaviour of tidal turbine blades. Thereafter, a global fatigue analysis methodology is proposed, which takes into account realistic operational loads in a tidal turbine environment. The global methodology is composed of sub-scale methodologies, which are validated through data obtained from experiments and from available literature.

1.1 ABBREVIATIONS & DEFINITIONS

BEMT	Blade Element Momentum Theory
BV	Bureau Veritas
CFD	Computational Fluid Dynamics
CFL	Constant Fatigue Life
CLD	Constant Life Diagrams
DNVGL	Det Norske Veritas – Germannischer Lloyd
FEA	Finite Element Analysis
FEM	Finite Element Method
FLD	Fatigue Life Diagram
IEC	International Electrotechnical Commission
IFREMER	Institut français de recherche pour l'exploitation de la mer
S-N	Stress vs Number of Cycles
UD	Uni-directional

1.2 REFERENCES

[1] W. V. Paepegem and J. Degrieck, “A new coupled approach of residual stiffness and strength for fatigue of fibre-reinforced composites,” *International Journal of Fatigue,* no. 24, pp. 747-762, 2002.

[2] J. Degrieck and W. V. Paepegem, “Fatigue damage modelling of fibre-reinforced composite materials: review,” *Applied Mechanics Review,* vol. 4, no. 54, pp. 279-300, 2001.

[3] C. Rubiella, C. A. Hessabi and A. S. Fallah, “State of the art in fatigue modelling of composite wind turbine blades,” *International Journal of Fatigue,* no. 117, pp. 230-245, 2018.

[4] T. Westphal and R. P. L. Nijssen, “Fatigue life prediction of rotor blade composites: Validation of constant amplitude formulations with variable amplitude experiments,” *Journal of Physics,* no. 555, 2014.

[5] A. t. Have, “WISPER and WISPERX : final definition of two standardised fatigue loading sequences for wind turbine blades,” 1992.

[6] B. Bulder, J. Perringa and e. al, “NEW WISPER - Creating a New Standard Load Sequence From Modern Wind Turbine Data,” 2004.

[7] R. P. L. Nijssen and T. Westphal, "Upwind Deliverable 3.1.7: Randomising New Wisper - Development and implementation of a method for rainflow equivalent randomisation of variable amplitude sequences -, Upwind".

[8] D. Caous, C. Bois, J.-C. Wahl, T. Palin-Luc and J. Valette, "Analysis of Mulit-axial Cyclic Stress State in a Wind Turbine Blade," in *20th International Conference on Composite Materials*, Copenhagen, 2015.

[9] Bureau Veritas, "NI603 - Current and Tidal Turbines," 2015.

[10] Det Norske Veritas - Germannischer Lloyd, DNVGL-ST-0164 Tidal Turbines, 2015.

[11] International Electrotechnical Commission (IEC), "Part 2: Marine energy systems: Design Requirements," in *IEC TS 62600-2*, Geneva, 2019.

[12] R. Nijssen, "Fatigue life prediction and strength degradation of wind turbine rotor," Delft University of Technology, 2007.

[13] C. Bathias, "An engineering point of view about fatigue of polymer matrix composite materials," *International Journal of Fatigue,* vol. 28, pp. 1094-1099, 2006.

[14] Bureau Veritas, NR546 - Hull in Composite Materials and Plywood, Material Approval, Design Principles, Construction and Survey, DT R02 ed., Paris: Bureau Veritas, 2018.

[15] Bureau Veritas Marine & Offshore, "Bureau Veritas Software," 2020. [Online]. Available: https://marine-offshore.bureauveritas.com/software.

[16] P. P. Camanhoa, C. G. Davila, S. T. Pinho, L. Iannucci and P. Robinson, " Prediction of in situ strengths and matrix cracking in composites under transverse tension and in-plane shear," *Composites,* vol. Part A (37), pp. 165-176, 2006.

[17] R. Talreja, "Assessment of the fundamentals of failure theories for composite," *Composites Science and technology,* no. 105, pp. 190-201, 2014.

[18] P. Soden, A. Kaddour and M. Hinton, "Recommendations for designers and researchers resulting from the world-wide failure exercise," *Composites Science and Technology,* no. 64, pp. 589-604, 2004.

[19] Z. Hashin and A. Rotem, "A Fatigue Failure Criterion for Fiber Reinforced Materials," *Journal of Composite Materials,* vol. 7, pp. 448-464, 1973.

[20] R. Talreja and J. Varna, Modeling Damage, Fatigue and Failure of Composite Materials, Woodhead Publishing, 2016.

[21] K. W. Garrett and J. E. B. , "Multiple transverse fracture in 90° cross-ply laminates of a glass fibre-reinforced polyester," *Journal of Materials Science,* no. 12, pp. 157-168, 1977.

[22] S. Ogin, P. Smith and P. Beaumont, "Matrix Cracking and Stiffness Reduction during the Fatigue of a (0/90)s GFRP Laminate," *Composites Science and Technology,* no. 22, pp. 23-31, 1985.

[23] N.-S. Cheng, "Power-law index for velocity profiles in open channel flows," *Advances in Water Resources,* no. 30, pp. 1775-1784, 2007.

[24] RealTide Project, "D3.1 - Generalised Tide-to-Wire model," RealTide Consoritum, 2019.

[25] International Association of Classification Societies, "IACS Rec. No.56 - Fatigue Assessment of Ship Structures," IACS, 1999.

[26] J. P. Tomy, L. Mouton, S. Paboeuf, A. Comer, A. Haldar and A. Portela, "Analytical Approach for Global Fatigue of Composite-hull vessels," in *MARTECH (yet to be published)*, Lisbon, 2020.

[27] V. A. Riziotis and S. G. Voutsinas, "Fatigue loads on wind turbines of different control strategies operating in complex terrain," *Journal of Wind Engineering and Industrial Aerodynamics,* no. 85, pp. 211-240, 2000.

[28] H. E. Kadi and F. Ellyin, "Effect of stress ratio on the fatigue of unidirectional glass fibre/epoxy composite laminae," *Composites,* vol. 25, no. 10, pp. 917-924, 1994.

[29] H. Mahfuz, M. Maniruzzaman, J. Krishnagopalan, A. Haque, M. Ismail and S. Jeelani, "Effects of stress ratio on fatigue life of carbon-carbon composites," *Theoretical and Applied Fracture Mechanics,* no. 24, pp. 21-31, 1995.

[30] D. B. Marghitu, C. Diaconescu and B. Ciocirlan, "Chapter 3: Mechanics of Materials," in *Mechanical Engineer's Handbook*, Academic Press Series in Engineering, 2001.

[31] K. B. Katnam, I. Aschroft and H. Khoramishad, "Load Ratio Effect on the Fatigue Behaviour of Adhesively Bonded Joints: An Enhanced Damage Model," *Journal of Adhesion,* 2010.

[32] H. Sutherland and J. F. Mandell, "Optimized Constant-Life Diagram for the Analysis of Fiberglass Composites Used in Wind Turbine Blades," *Journal of Solar Energy Engineering,* vol. 127, pp. 563-569, 2005.

[33] A. Vassilopulos, B. Manshadi and T. Keller, "Influence of the constant life diagram formulation on the fatigue life prediction of composite materials," *Internationla Journal of Fatigue,* no. 32, pp. 659-669, 2010.

[34] N. L. Post, S. W. Case and J. J. Lesko, "Modeling the variable amplitude fatigue of composite materials: A review and evaluation of the state of the art for spectrum loading," *International Journal of Fatigue,* no. 30, pp. 2064-2086, 2008.

[35] A. P. Vassilopoulos, B. D. Manshadi and T. Keller, "Piecewise non-linear constant life diagram formulation for FRP composite materials," *International Journal of Fatigue,* no. 32, pp. 1731-1738, 2010.

[36] ISO, "ISO 527-1:Plastics — Determination of tensile properties," 2019.

[37] RealTide, "Effect of sea water aging on the static and fatigue properties of composites for tidal blade design," RealTide Consortium, 2019.

[38] M. Arhant, P. Davies, S. Paboeuf and E. Nicolas, "Reliability of Composite Tidal Turbine Blades," in *22nd International Conference on Composite Materials*, Sydney, 2019.

[39] M. Kawai and N. Itoh, "A failure-mode based anisomorphic constant life diagram for a unidirectional carbon/epoxy laminate under off-axis fatigue loading at room temperature," *Journal of Composite Materials,* vol. 48, no. 5, pp. 571-592, 2014.

[40] S. Abrate, "Matrix Cracking in Laminated Composites: A Review," *Composites Engineering,* vol. 1, no. 6, pp. 337-353, 1991.

[41] R. Nijssen, D. v. Delft, P. Joosse, A. v. Wingerde, C. W. Kensche, T. P. Philippidis, P. Brøndsted and A. Dutton, "Optimat Blades - Optimal and Reliable Use of Composite Materials for Wind Turbines," OPTIMAT Project.

2 STATE-OF-THE-ART FATIGUE ASSESSMENT OF MARINE COMPOSITE STRUCTURES

The evolution of fatigue on composites is not linear in nature. For vast majority of fibre-reinforced composite materials, the fatigue evolution can be divided into three stages, as can be seen in Figure 1 [1]. An initial phase with a rapid stiffness reduction is followed by an intermediate region with approximately linear reduction in stiffness. The final stage is characterised by stiffness reduction in abrupt steps, ending in specimen fracture. The paper further investigates on how these three stages of stiffness degradation can be modelled.

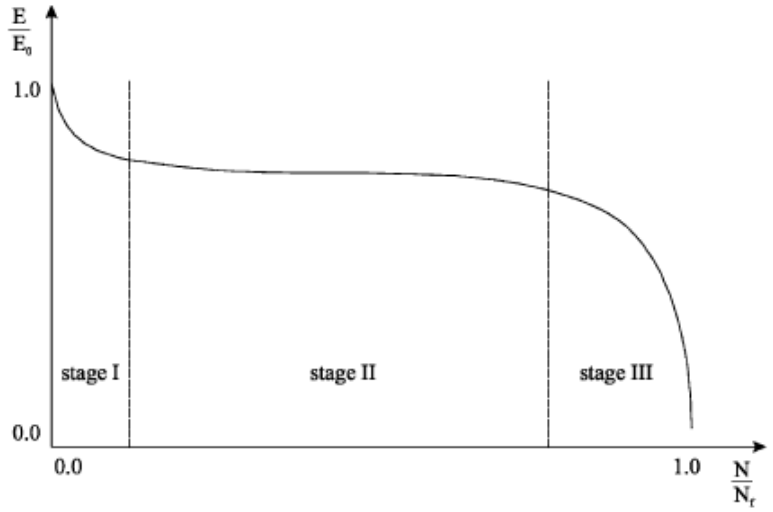

Figure 1: Typical evolution of stiffness over the course of fatigue life of a wide range of fibre-reinforced composite materials

2.1 FATIGUE MODELLING APPROACHES

Three fatigue modelling approaches for fibre-reinforced polymers can be distinguished [2]. In an increasing order of complexity, as well as accuracy in representing the fatigue evolution mechanism, these are: (i) fatigue life models, which use S-N curves or Fatigue Life Diagrams (FLDs) and predict only the final failure of the material; (ii) phenomenological models, which describe the fatigue evolution in terms of an empirical relationship with a phenomena such as stiffness degradation; and (iii) progressive damage models, which use one or more damage variables, such as matrix cracks, to quantify the extent of damage at each iteration. A schematic diagram showing the various approaches is presented in Figure 2, wherein the most basic model is placed at the base of the pyramid.

The classical approach to develop a fatigue damage model is by using the S-N curve approach. This is the most basic fatigue damage model, based on the fatigue life of the material. It does not take into account the actual damage mechanism; the fatigue life of the material is experimentally computed for different stress ranges, and the same is then plotted as an S-N curve which represents the fatigue performance of the material. The computations are much simpler and efficient in terms of computational time and effort.

While considering anisotropic materials such as multi-layer composite laminates, the actual mechanism involved is much more complex than that would be for a homogeneous, isotropic material like metals. The interaction between the composite layers can mean that, even if one ply is damaged, the rest of the plies can take extra load. The gradual deterioration in a fatigue damage leads to a

continuous redistribution of stresses. Moreover, within a single ply, the fibre and the resin behaviour are entirely different, making it difficult to extend the results from one load case to another.

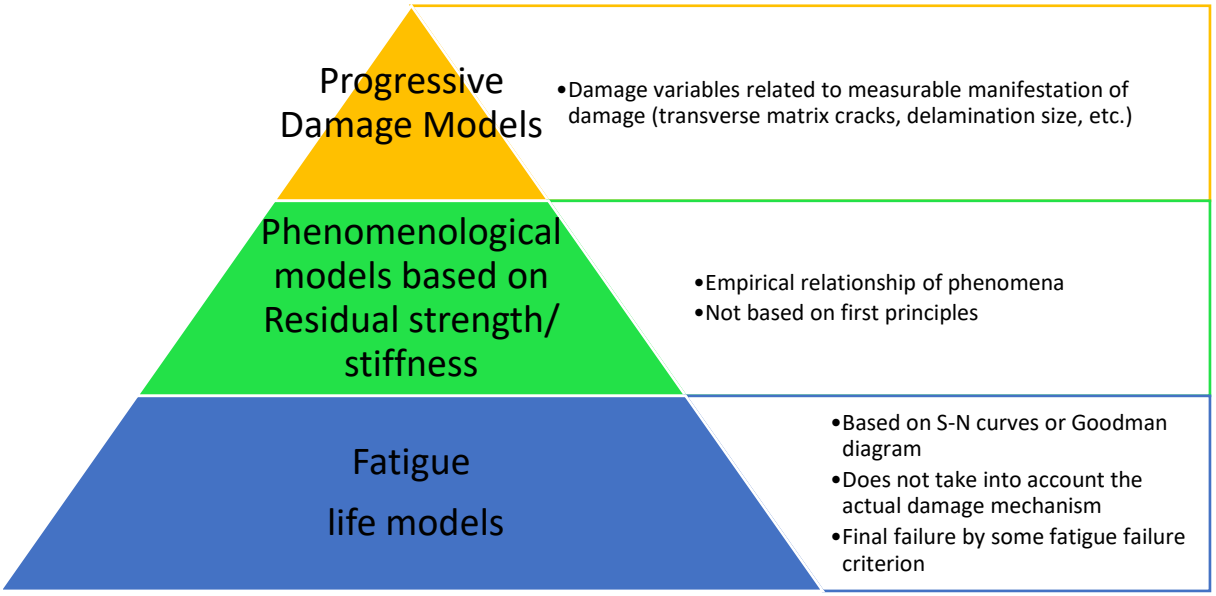

Figure 2: Fatigue Modelling Approaches

2.2 MODELLING MULTI-AXIAL FATIGUE

The fatigue state in composite laminates is a multi-axial phenomenon - even with an orthotropic assumption. Phenomenological models and progressive damage models take into account the fact that the prediction of the evolution of fatigue of the composite structure depends on the 'path' of successive damage states. Using such models allows the state of fatigue during each computational iteration to be identified.

However, the procedure requires to simulate each loading cycle numerically. In a layered and non-homogeneous structure such as the blade of a tidal turbine, multi-axial fatigue analysis using such models becomes non-realistic and computationally non-feasible to apply. When considering that the minimum fatigue life expected for these application cases falls in the range of 10^9 cycles, such computations become cumbersome, computationally expensive and impractical at the preliminary design stage.

In fatigue design of materials, it is not necessary to understand and follow this 'path' of successive damage states. More importantly, the designer needs to have an idea about the number of cycles that the structure can withstand, when subjected to a sequence of fluctuating stresses. In reality, uncertainty factors which affect the fatigue behaviour are not accounted by any analytical and numerical simulations of the fatigue phenomenon. Some of these uncertainty factors include ageing effects, uncertainty in determining the loads, and uncertainty in manufacturing processes.

Thus, the objective for fatigue design of tidal turbine blades should be to have a methodology that is more analytically developed than the classical S-N curve, but not as computationally intensive as the phenomenological models. The approach proposed within this report intends to fall in between these two categories.

2.3 LOADING CONDITIONS FOR TURBINE BLADES

A globally accepted framework for fatigue analysis of composite materials does not exist at the time of drafting this document. This is the case even for constant amplitude fatigue loadings. Tidal turbine blades are exposed to loads with varying amplitudes and intensities throughout their service life. Moreover, the laminates experience a cyclic stress state that is multi-axial in nature. For these reasons, literature on fatigue loading conditions of tidal turbines is practically non-existent. Task 1.4 of the RealTide project aims to address this gap as well.

The nature of forces experienced by tidal turbines can be thought of as similar to that of wind turbines. The wind turbine industry, is relatively well established with a good amount of literature on the blade forces. Fatigue loading of wind turbine blades is still a novel topic; however, there are certain investigative studies conducted in this aspect. Rubiella et al [3] provide a comprehensive summary about the state of the art in fatigue modelling of composite wind turbine blades. The various fatigue models that could be implemented for basic fatigue considerations are discussed within this paper.

Fatigue load spectrum characterisation for wind turbine blades is also an ongoing research topic. From the work of Westphal and Nijssen [4], it is understood that the use of Wisper and WisperX spectra [5] is predominant in the wind turbine industry, as they were derived from strain measurements on wind turbine blades in operation. Recent European research projects such as OPTIMAT and Upwind have resulted in improved spectra such as the 'NEW WISPER' [6] and 'NewWisper2' [7].

The evaluation of fatigue loads by analytical methods is more challenging. Caous et al [8] proposed to consider the multiaxial cyclic stress state on a wind turbine blade by computing the stresses along the principal axes. The idea behind using the principal stress approach is to reduce the problem into a biaxial stress state. Thereafter, the biaxial fluctuating load is represented by the ratio between the stresses in the two directions – the mean stress, the stress amplitude, the phase shift, and the aspect ratio of the ellipse representing the stress state.

2.4 SAFETY COEFFICIENT IN DESIGN

The design of a tidal blade is governed by the accuracy in simulating and predicting the stresses that it is expected to encounter during its service life. The complexity in simulating such a real-life environment leads to uncertainties in the estimation of the design criteria. Designers and classification societies account for this uncertainty by using safety coefficients in design; thereby increasing the design scantling to account for any errors in the determination of the design conditions and material properties.

In recent structural applications, the use of a partial safety factor approach is prevalent among all Classification societies. The partial safety factor method is a design method by which the target safety level is obtained as closely as possible by applying load and resistance factors to characteristic values of the governing variables and subsequently fulfilling a specified design criterion expressed in terms of these factors and these characteristic values. The governing variables consist of:

- loads acting on the structure or load effects in the structure
- resistance of the structure or strength of the materials in the structure.

Depending on the type of design loads considered (e.g. Operational Loads, Environmental Loads, Fatigue Loads, etc.), classification societies provide partial safety factors that need to be considered in the design. Similarly, the partial safety factors related to the material (i.e. composites, in the current

context) can vary depending on the manufacturing process, ageing effect, etc. Existing regulations for tidal turbine blades are found in:

- Bureau Veritas (BV) Guidance Note for Current and Tidal Turbines – NI603 [9]
- Det Norske Veritas – Germannischer Lloyd (DNVGL) Standard for Tidal Turbines – DNVGL-ST-0164 [10]
- International Electrotechnical Commission (IEC) Technical Specification for Marine Energy systems – IEC TS 62600-2 [11]

Table 1 lists categories and sub-categories of the partial safety factors considered by the three different above regulations for fatigue strength evaluation. It may be noted that the partial safety factor for fatigue loads is taken as 1.0 for all regulations, underlining a good confidence in the fatigue load determination. However, the various components of the material partial safety factors are defined differently. The detailed description of the partial safety factors is omitted for brevity. The values for the different partial safety factors are not provided here, and they can be found in the respective standards. However, the uncertainty in fatigue strength evaluation can be highlighted by the fact that the combination of the different partial safety factors can give a total safety factor as high as 30 for extremely severe design conditions.

Table 1: Partial safety factors for fatigue strength evaluation

Category	Sub-Category
Material	Manufacturing Method
	Curing Process
	Material degradation – Ageing
	Environmental conditions – Temperature, humidity
	Sandwich or Monolithic construction
	Uncertainty in test values of mechanical properties
Loads	Load determination
	Type of load carried by fibres or core – Tensile/Compressive/ Shear
	Combined Stresses
	Buckling
	Operating Condition of turbine
	Component accessibility, inspection and maintenance
	Risk of failure

3 FATIGUE ASSESSMENT METHODOLOGY

During the design stage of a tidal turbine, the fatigue strength assessment of the blades is paramount in defining the structural scantling. The fatigue assessment should be indicative about the proposed durability of the structure. However, with the definition of the forces on the blades being a complex task in itself, and with the design of the blade scantlings being an iterative process, the fatigue assessment chiefly borders on a predictive approach. The objective during the design stage is to avoid additional computational effort - the prediction of precise loads is not important, as long as the order of magnitude of the predicted loads are within an acceptable uncertainty level. In any case, some uncertainties, such as those due to environmental conditions, cannot be avoided regardless of the prediction precision achieved. The uncertainties in the evaluation procedure are accounted for by using adequate safety factors.

Considering these requirements, and in line with the current industry practice, the fatigue assessment methodology proposed is based on the classical fatigue life models. Based on other works in the literature, the use of fatigue life models, such as S-N curves and Constant Life Diagrams, to estimate fatigue behaviour of composites is limited [12]. A progressive damage model, that serves to predict the crack initiation, propagation, until the final failure of the laminate, is deemed to be computationally intensive for the complex loading environment of a tidal turbine blade. It is therefore proposed to add certain aspects of a phenomenological approach, to include correlation with the actual damage mechanisms of composite materials. With reference to Figure 1, the major stage in the fatigue evolution on a composite laminate is the crack propagation stage. Hence, it would be valuable to enhance the classical fatigue-life models, with the inclusion of effects from this stage of the fatigue evolution. Within the fatigue assessment methodology proposed, such an enhancement is made by evaluating the residual stiffness of the laminate during its service life.

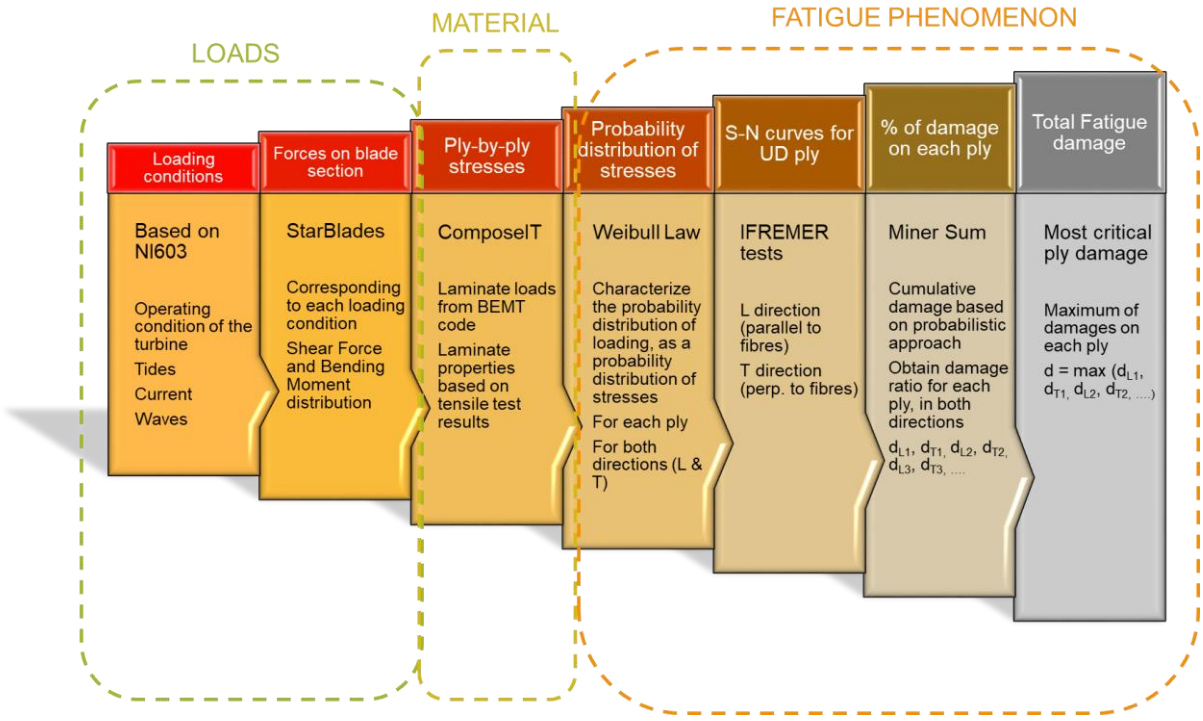

Figure 3: Global Fatigue Analysis Methodology for Tidal Turbine Blades

A schematic diagram illustrating the proposed global fatigue analysis methodology is shown in Figure 3. The fatigue methodology aims to address the three main complexities associated with the fatigue evaluation problem for a tidal turbine blade – namely, the complexities in the loads, the material and the description of the fatigue phenomenon. In fact, the literature review presented in Section 2 provides an understanding about each of these complexities (Sections 2.3, 2.2, 2.1 respectively). The various segments of the method, which specifically address these complexities are also highlighted within the schematic.

The subsequent sections aim to address the various blocks of the global methodology. First, the ply-by-ply approach to evaluate the fatigue for a composite laminate is explained (Section 3.1) – this addresses the complexity of the material, and proposes a way to include it within the fatigue evaluation process. The ply-by-ply approach is explained for a constant amplitude loading case, for ease of explanation. Thereafter, the fatigue evaluation procedure is described in Sections 0 and 3.3, which include explanations about how the phenomenological models are combined with the fatigue life models. Finally, the complexities in the loads are addressed, by considering a long-term distribution of the expected fatigue loads on the turbine blades (Section 3.4).

3.1 PLY-BY-PLY APPROACH TO EVALUATE FATIGUE STRESSES

The characterisation of fatigue behaviour for composite laminates usually requires multi-variant analysis unlike metallic fatigue [13]. The behaviour can be different according to the stress ratio, the laminate configuration (stacking sequence) and the failure mode. A comprehensive fatigue life model that captures all these variations would need to be characterized by S-N curves for multiple stress ratios or by a Constant Life Diagram. Such a characterization would require an intensive experimental campaign. Moreover, as the behaviour is different for each stacking sequence within a turbine blade, such a characterization is impractical from a design perspective.

In static analysis of composite materials, the globally used method is the ply-by-ply analysis, wherein the anisotropy of the laminate description is considered by using an orthotropic simplification. All the mechanical properties of the composite laminate can be simplified into three orthogonal planes – parallel to the fibre direction (L-direction), perpendicular to the fibre direction (T-direction) and through the thickness of the laminate (N-direction) (see Figure 4). While considering unidirectional plies, the properties in the L-direction are dominated by the fibres, and those in the T-direction and N-direction by the matrix.

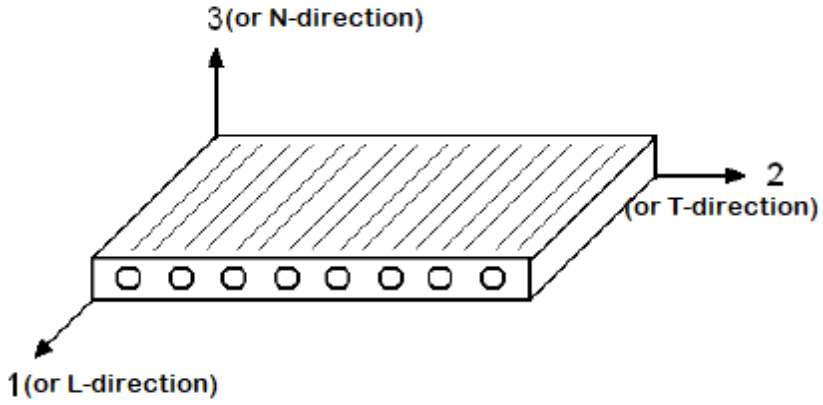

Figure 4: Composite laminate orthogonal axes

A ply-by-ply analysis methodology defines the behaviour of each ply (or layer) within the laminate separately. The individual stresses on each layer depend on the mechanical properties (moduli) of the particular layer, its position in the laminate thickness and the global strain of the laminate. For each ply, the elastic stresses in the L and T directions as well as the shear stress in the L-T plane can be thus obtained. This gives the two-dimensional stress state of the ply, which can subsequently be used to determine its mechanical behaviour. This kind of design philosophy is used for static analysis of composite laminates (for example NR546 BV Rules for Composite Materials [14]), and the idea is to extend such an approach for cases when the laminate is subjected to fluctuating stresses, i.e. for fatigue loading.

This section provides an outline of the proposed analytical methodology to evaluate the fatigue of a composite laminate under any given loading, using the ply-by-ply approach. Subsequently, in Section 3.4, the methodology is extended to include the complex loading histogram experienced by a composite blade under realistic operational conditions.

3.1.1 Fibre and matrix stresses

For any given laminate load (bending moment or axial loads), the stresses on each ply in the stacking sequence can be obtained using composite macro-mechanical tools. Such tools predict the stresses in the L-T plane: σ_1 (axial force along the fibre direction), σ_2 (axial force perpendicular to the fibre direction), and τ_{12} (in-plane shear). Within the evaluation studies performed as part of this report, ComposeIT, a freeware developed by Bureau Veritas [15], is used for this purpose.

Within the global fatigue analysis methodology, it is required to analyse the fatigue effect on the fibre and matrix separately. In particular, this would help to separately analyse phenomena such as matrix cracking and fibre failure. Therefore, for each lamina, the ply-by-ply stresses are further resolved to obtain equivalent fibre and matrix stresses ($\sigma_{f(eq)}$ and $\sigma_{m(eq)}$ respectively) at the ply level.

From the orthotropic simplification, σ_1 can be considered as acting only on the fibres, and σ_2 can be considered as acting only on the matrix. The in-plane shear, τ_{12}, would have an impact on both the fibre and the matrix, and needs to be investigated separately.

The combined effect of in-plane shear and transverse tensile stresses in facilitating matrix cracking is known in the literature, from sources such as [16]. This is also evident from the considerations of various failure theories for composite materials under multi-axial loading, such as the Tsai-Hill, Tsai-Wu and Hashin criteria [17]. These failure criteria are usually characterized by 3D failure envelopes in a σ_1-σ_2-τ_{12} coordinate system. As the consideration here is to evaluate the matrix cracking, only the σ_2-τ_{12} plane is considered.

The comparison between the experimentally measured failure stresses and the predicted failure stresses based on various failure theories are shown in Figure 5 [18]. These are plotted on the σ_2-τ_{12} plane, and it can be seen that the general trend for most of the theoretical formulations is to have an elliptical failure envelope. Such an elliptical relation is used to derive an equivalent value of the matrix stress for a combined multiaxial loading of σ_2 and τ_{12}.

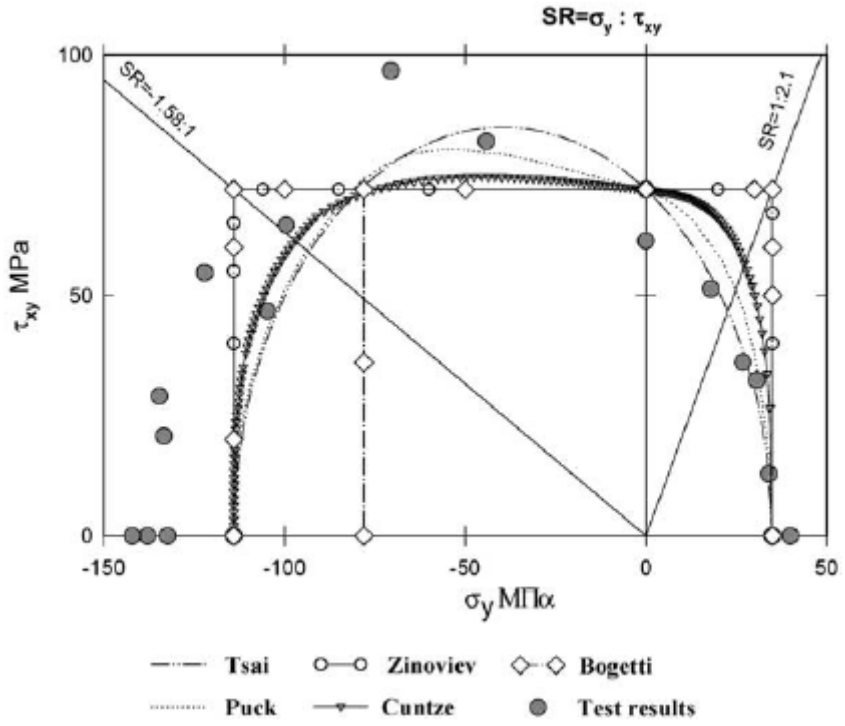

Figure 5: Composite failure envelope in the σ_2-τ_{12} plane [18]

The elliptical failure envelope is defined as shown in Figure 6. The extremes of the major axes of the ellipse are defined by the failure states when acted upon only by σ_2. These points correspond to the ultimate tensile and compressive strengths of the ply in the T direction (or direction 2), i.e. S_{2T} and S_{2C} respectively. Similarly, the minor axis can be defined by the ultimate in-plane shear strength, S_{12}. Knowing the four corners of the ellipse, the failure envelope (black solid line) can be defined. In fact, the 'elliptical' failure envelope is defined by two different ellipses, corresponding to the left and right halves respectively in the plane.

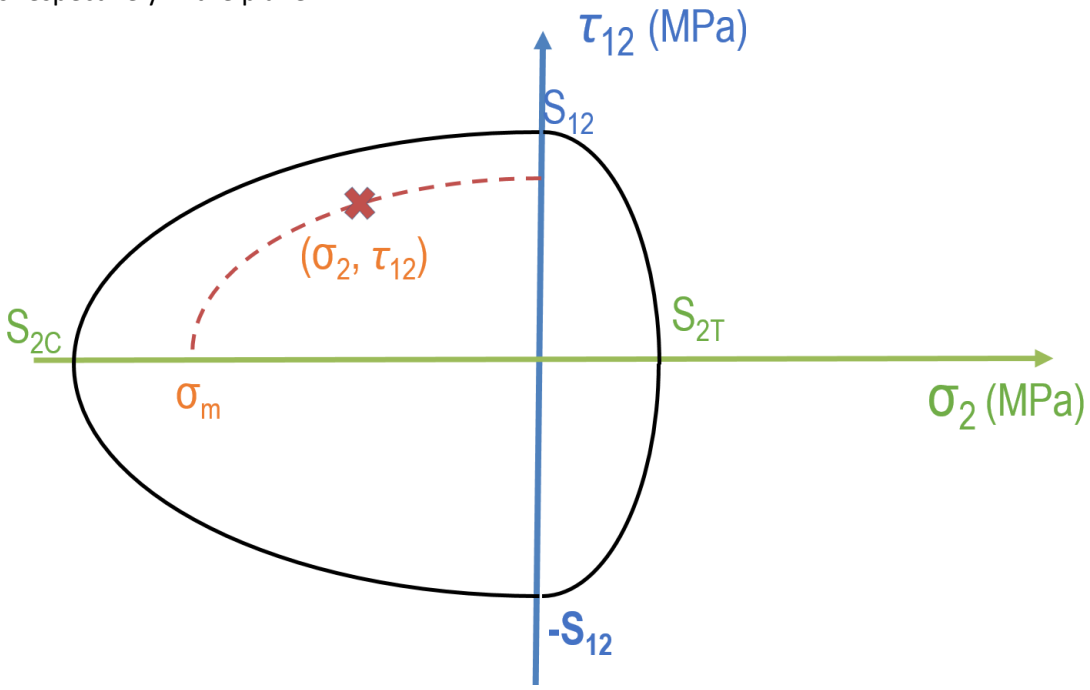

Figure 6: Equivalent ply level matrix stress for multi-axial loading

Now, it is presumed that, a quarter-ellipse traced in the same quadrant following the equation of the failure envelope ellipse (red dotted line) represents stress states that correspond to the same damage level. Therefore, for any given biaxial stress state (σ_2, τ_{12}), an equivalent augmented stress in direction 2 can be computed, which accounts for the in-plane shear effect. In the diagram, this is represented as σ_m and this is used as the equivalent stress acting on the matrix at the ply level. Mathematically, this can be computed as:

$$\sigma_{m(eq)} = \sqrt{\sigma_2^2 + (f_2\tau_{12})^2}, \text{ where } f_2 = \begin{cases} \frac{S_{2T}}{S_{12}} & for\ right\ half \\ \frac{S_{2C}}{S_{12}} & for\ left\ half \end{cases} \quad \text{..... Eq. 1}$$

Here the factor f_2 is used to represent the ratio between the ultimate strength in the T direction and the ultimate shear strength. Depending on the quadrant under consideration, the value of S_2 used would change between S_{2C} and S_{2T}, and the value for S_{12} could be positive or negative. Eventually, $\sigma_{m(eq)}$ has an absolute value always greater than σ_2.

In the fibre-dominated L-direction, the equivalent stress is taken as equal to the stress along direction 1. That is to say, the effects of σ_2 and τ_{12} are ignored for the fibre equivalent stress. Therefore,

$$\sigma_{f(eq)} = \sigma_1 \quad \text{..... Eq. 2}$$

A similar formulation has been used by Hashin and Rotem [19] while considering the fatigue failure of off-axis plies. The actual formulation from any of the failure theories could be used in the derivation of this equivalent matrix stress. The conceptual understanding of the equivalent matrix stress would remain the same. However, this would result in a much more complicated equation for the equivalent matrix stress; and thus, it is assumed that the elliptical failure envelope gives a reasonably accurate prediction.

3.2 RESIDUAL MATRIX STIFFNESS AND AUGMENTED FIBRE STRESSES

The mechanism for progressive fatigue failure of laminates commences with matrix cracking, as described in Chapter 2.2.2.2 of '*Modeling Damage, Fatigue and Failure of Composite Materials*' [20]. The matrix cracking would cause a reduction in the laminate stiffness, and consequently a change in the slope of the stress-strain curve is observed. This has been observed experimentally; Figure 7 shows an example from the work by Fraser Cossens, extracted from [20]. The increased strain due to the stiffness reduction can induce an increased stress on the fibres – as the matrix cracking only reduces the matrix stiffness, and the fibre stiffness is assumed to remain intact. As matrix cracking progresses, thus it can be considered to have a progressive increase in the stresses experienced by the fibres, at the ply level.

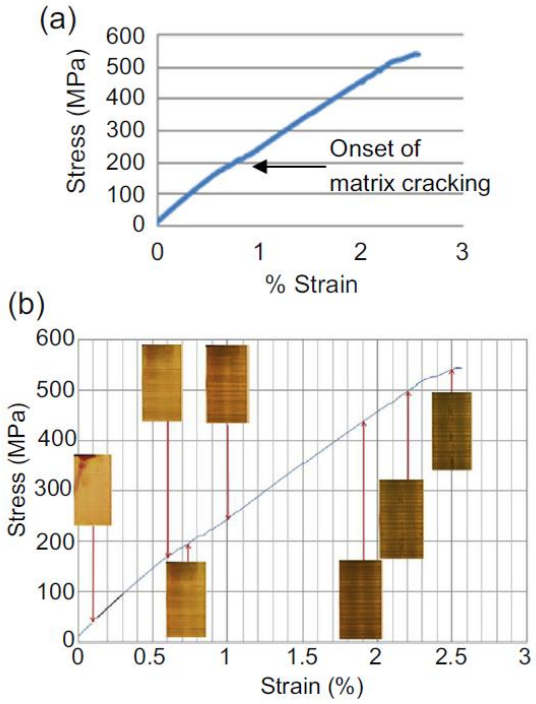

Figure 7: (a) Typical stress-strain curve for a cross-ply laminate with accumulating matrix cracks. (b) Crack accumulation in a transparent GFRP cross-ply laminate

In order to analytically formulate this hypothesis, it is required to link the extent of matrix cracking to the number of cycles during the fatigue loading. Within the literature, the usual procedure is to describe the stiffness reduction as a function of the average crack density or the crack spacing [21]. While this link is more logical, in order to facilitate the utility within a fatigue analysis, it is required to express the stiffness reduction as a function of the number of cycles. Such a link was established by Ogin et al. [22] with an expression for the rate of change of stiffness (*dE/dN*):

$$-\frac{1}{E_0}\cdot\frac{dE}{dN} = A\left[\frac{\sigma_{max}^2}{E_0^2\left(1-\frac{E}{E_0}\right)}\right]^n \qquad \text{..... Eq. 3}$$

Where E_0 = Young's modulus of the uncracked composite
σ_{max} = Maximum stress in the constant-amplitude fatigue cycle
E = Stiffness after any given number of cycles (N)

A, n = Constants determined experimentally

Integration of equation 3 gives the instantaneous stiffness of the laminate as a function of the number of cycles:

$$E(N) = E_0 * \left[1 - \left(\frac{A}{k}\right)^k \left(\frac{\sigma_{max}^2}{E_0^2}\right)^{1-k} N^k\right] \quad \text{..... Eq. 4}$$

Where *k* = Constant, defined as 1/(n+1)

This expression is experimentally validated for $[0/90]_{2s}$ specimens in the literature [22]. This can be extended to the unidirectional plies as well, without any loss of generality. If the cyclic fluctuation of stresses within one cycle is treated quasi-statically, then the equivalent strain on the ply can be obtained as:

$$\varepsilon_{ply} = \varepsilon_{fibre} = \varepsilon_{matrix} = \frac{\sigma_{max}}{E(N)}$$

With the assumption that the fibre deforms elastically, the increase in fibre stress, after each cycle, can thus be expressed as:

$$\sigma_f(N) = E_f * \varepsilon_f = \frac{E_f * \sigma_{max}}{E_0 * \left(1 - \left(\frac{A}{k}\right)^k * \left(\frac{\sigma_{max}^2}{E_0^2}\right)^{1-k} N^k\right)} \quad \text{..... Eq. 5}$$

Thus, by knowing the values of the constants *A* and *k*, the equation provides a relation that characterizes the gradual increment in stresses experienced by the fibre, due to the accumulation of matrix cracks.

In the classical S-N curve, the number of cycles to failure is obtained by the intersection of the curve with a horizontal line (parallel to the N-axis) at the maximum cyclic stress (σ_{max}). This equation provides a curvilinear path to follow, at a given σ_{max} based on a phenomenological model. From an S-N curve referential, such a model would predict an earlier fibre failure, by accounting for the gradual accumulation of matrix cracks (see Figure 8).

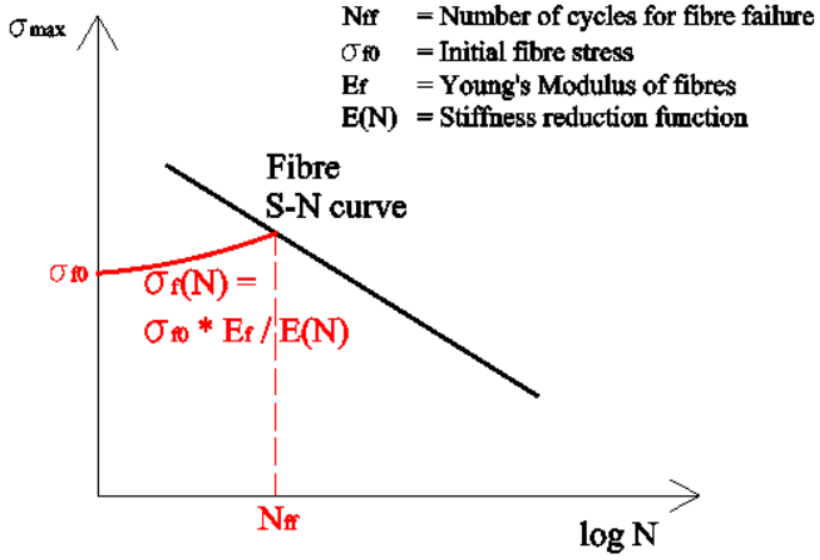

Figure 8: Illustration of augmented fibre stress due to matrix cracking

3.3 EVALUATION OF FATIGUE LIFE USING UD S-N CURVES

Section 3.1 proposed a hypothesis on how to evaluate the equivalent fibre and matrix stresses at the ply level. The advantage of having ply level stresses is that the data for fatigue of UD fibres can be used to determine the damage. An evaluation using S-N curves is not direct, as the phenomena of matrix cracking and fibre failure are not completely independent of each other. An expression that links the accumulated matrix cracking to an increase in fibre stresses was presented in Section 3.2. The subsequent paragraphs provide a framework that implements the use of the fibre and matrix stresses in determining the fatigue life of a laminate with a given stacking sequence.

3.3.1 Procedure

The procedure for fatigue life evaluation revolves around the classical S-N curve concept. As the S-N curve is a material characteristic, it is different for different laminate stacking sequences. The impracticality of characterising the S-N curve for every laminate in the blade design leads to an approach that is more focused on the micromechanics of the composite laminate. This method proposes to evaluate fibre fatigue and matrix fatigue separately. The evaluation of the equivalent fibre and matrix stresses is provided in Section 3.1.1.

The procedure for evaluation of fatigue life is enumerated below. Figure 9 illustrates a graphical summary of the procedure.

i. For any given composite laminate, calculate the ply-by-ply stresses (σ_1, σ_2 and τ_{12}) for the maximum load in a fatigue cycle (F_{max}), using macromechanical laminate analysis tools (for example, ComposeIT [15]).
ii. Calculate the fibre and matrix stresses. The initial fibre stress (σ_{f0}) as $\sigma_{f0} = \sigma_1$. Stress on matrix (σ_m) is calculated as a combined effect of σ_2 and τ_{12}, using Equation 1 (see Page 14).

$$\sigma_{f0(eq.)} = \sigma_1$$
$$\sigma_{m(eq.)} = \sqrt{\sigma_2^2 + (f_2\tau_{12})^2}, \text{ where } f_2 = \frac{S_2}{S_{12}}$$

iii. Fatigue of matrix: Compare the σ_m value with the S-N curve for matrix (tensile or compressive) to compute the number of cycles for matrix damage (N_{fm}).
iv. Fatigue of fibres: To evaluate the number of cycles to fibre failure (Nff), trace the path of σ_f according to Equation 4, starting from σ_{f0} (refer Figure 8).
v. The design number of cycles to failure can be decided as the minimum of N_{ff} and N_{fm}.

The fatigue life behaviour of the matrix is to be obtained from fatigue tests of UD [90] laminates. For these laminates, the fatigue behaviour is dominated by matrix cracking and fibre-matrix debonding. Similarly, the fatigue life behaviour of the fibres is obtained from the fatigue tests of UD [0] laminates. For such laminates, the fatigue loads would lead to eventual failure of the fibres.

It needs to be remarked that the experimental tests for fatigue characterisation of UD [0] laminates is performed with uniaxial loads along the fibre direction. Matrix cracking, leading to a loss in stiffness, is not expected during such tests. However, a realistic loading case would be multi-axial, and would lead to a progressive degradation of the matrix due to cracking. The implementation of augmented fibre stresses in step (iv) of the procedure above (according to Section 3.2) is expected to account for this gradual degradation of the laminate strength.

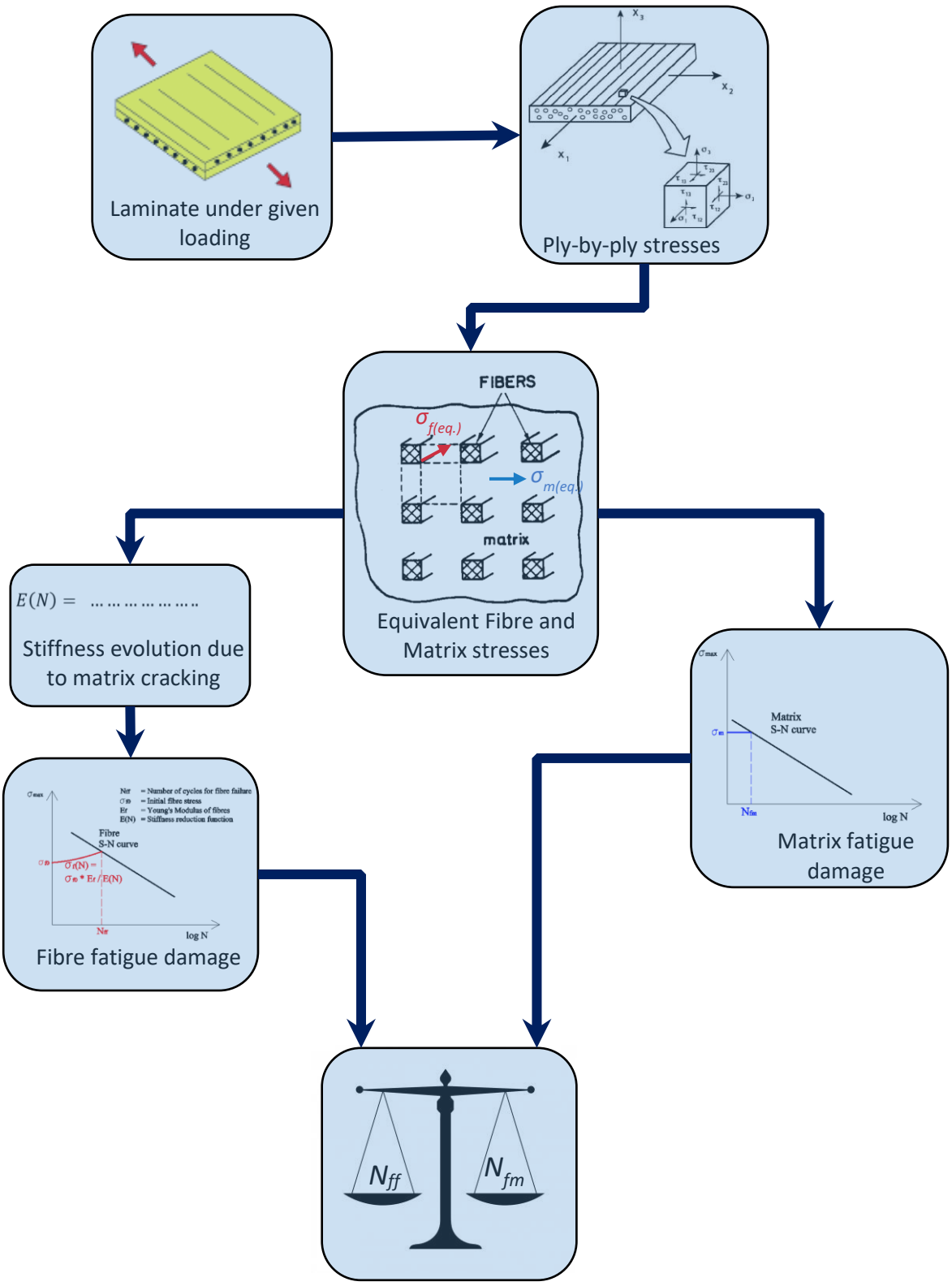

Figure 9: Procedure for fatigue life evaluation using UD S-N curves

Step (v) of the procedure prescribes to decide the design number of cycles as the minimum of N_{ff} and N_{fm}. In most practical loading cases, it is expected that the matrix cracking would be achieved first, i.e. $N_{fm} < N_{ff}$. Choosing this as the design point would lead to conservative designs, as the crack propagation within a multi-oriented laminate stacking sequence is restricted, as compared to the unidirectional ply. Nevertheless, N_{fm} would give an indication about the expected commencement of progressive crack propagation (stage III in Figure 1) of the laminate fatigue. As a further improvement to the methodology, N_{fm} could be not considered as the design point; but a further augmentation of the fibre stresses would need to account for this phase.

3.3.2 Assumptions in the Methodology

Some of the key assumptions used in the ply-by-ply fatigue analysis methodology, and the subsequent evaluation of fatigue life using UD S-N curves are as follows:

i. The static failure envelope for combined stress state (elliptical failure envelope for σ_2 vs τ_{12}) is assumed for fatigue failure too.
ii. Fibre fatigue and matrix fatigue are treated independently. The S-N curves for UD[0] and UD[90] laminates are assumed to be representative of the fibre fatigue and matrix fatigue respectively.
iii. The failure mechanism in a combined stress state is considered the same as that which would cause the failure for the UD [90] laminate, i.e. effects such as micro-buckling of fibres in compressive loads are not considered.
iv. Fatigue damage initiation is calculated as the point (number of cycles) where the first matrix crack is expected from the S-N curve analysis.
v. Inter-laminar shear effects are not accounted for.
vi. Fibre-matrix debonding is not accounted for.
vii. Time-dependent (creep) effects are ignored.

3.4 LONG-TERM STRESS DISTRIBUTION

The ply-by-ply stress evaluation methodology proposed earlier is based on the classical S-N curve approach for constant amplitude fatigue loading. For industrial applications, such as for tidal turbine blades, the fatigue loads are of varying amplitude, in accordance with the environment and the operating conditions. The methodology needs to be extended to adapt to such complex loading scenarios.

Long-term fatigue loads are usually represented as frequency histograms, showing the number of cycles corresponding to each stress level. The total fatigue damage is then estimated using the Palmgren-Miner rule, which assumes accumulation of fatigue damage on the material irrespective of the order in which the loading cycle is applied. For each level of stress range (i), the number of cycles endured within the service life (n_i) is read from the probability distribution function; and the number of endurable stress cycles (N_i) obtained from the S-N curve. The percentage of damage (d) on the ply, according to the Palmgren-Miner Rule is then:

$$d = \Sigma \, (n_i / N_i) \qquad \text{..... Eq. 6}$$

3.4.1 Fluctuating Forces on a Tidal Turbine

The load on the turbine is due to the fluid force acting on it while it rotates in the environment. The rotation of the turbine creates a distribution of fluid force along its length, and this causes a bending moment on the blades along the axial flow direction. If the turbine operates in a steady uniform flow field, with a constant rotational speed, this force distribution remains the same throughout its operation. However, in reality, this force distribution fluctuates due to:

i. variations in the inflow velocity (tides, waves, turbulence)
ii. variations in the flow environment (varying density, viscosity, etc.)
iii. variations in the rotational speed of the turbine.

Table 2: Force fluctuations on a tidal turbine blade

Factor	Time Period	Intensity	How to consider
Tidal flow	12 hours	2 (Reversal of stresses)	Sinusoidal fluctuations during the ebb-flow-ebb cycle
Turbine rotation	0.5 seconds	1/20	Considering operational profile of the turbine
Waves	10 seconds	1/8 (Reversal of stresses)	Requires analysis of irregular wave spectrum at the particular site
Turbulence	0.1 seconds	1/10	Requires CFD analysis
Varying density	Unknown	1/40	Depends on the temperature, salinity and location
Varying viscosity	Unknown	Unknown	Depends on the temperature, salinity and location
Geometry complexity	Unknown	Unknown	Requires CFD analysis to investigate the effect of nacelle, tower, etc.

An accurate analysis of the fatigue loads would need to consider all these types of fluctuations. Table 2 shows a brief description of these factors. To give an indication about the impact of each of these factors, approximate values of the time period and intensity of these fluctuations are also provided. These are only indicative values, intended to provide an order of magnitude. Time period gives an indication about the duration of each fluctuation, thereby giving an estimate about the expected

number of cycles during the service life. The intensity is measured as how much the fluctuation varies from a mean value – it is an approximate ratio of the amplitude of fluctuations (σ_{amp}) to the mean value (σ_{mean}).

The level of detail required in defining the fatigue load spectrum is the choice of the designer, after giving due consideration to the impact of each of these factors. The intensity mentioned in Table 2 could be used indicatively to understand their relative impacts. Description of methods to evaluate a combined long-term load distribution is not envisaged within this report. However, the following paragraphs provide brief descriptions about possible methods that could be employed to account for some of the major fluctuating stress components – namely the stress fluctuations due to tidal flow, turbine rotation and waves.

Tidal Flow: The variation in the inflow velocity could be characterized by sinusoidal fluctuations of the tidal stream velocity. The stress fluctuations would be ranging from the maximum value at the peak ebb tide, to the minimum value at the peak flow tide. As the tide directions invert during one cycle of 12 hours, such fluctuations would be represented by a negative stress ratio – alternating tension and compression. The frequency distribution can be obtained by generating a distribution of the tidal stream velocities at the site, and thereafter converting it into equivalent bending moment spectra and subsequently the stress spectra.

Turbine Rotation: The rotation of the turbine causes high frequency fluctuations of the stresses, in accordance with the rotation speed of the blade. The frequency of these fluctuations corresponds to the number of rotations made by the turbine during its lifetime. Such a frequency distribution can be generated, considering the expected operating profile of the turbine. Typically the blade experiences maximum stress when it is at its highest point and minimum stress when it is at its lowest point. To determine the stress range for each rotation, variation of the axial velocity profile along the depth of the sea could be considered.

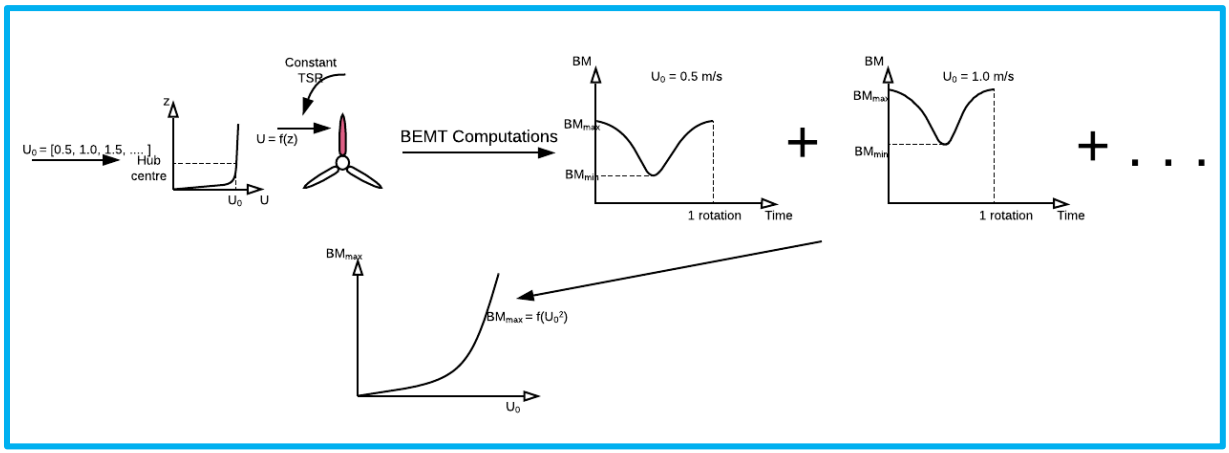

Figure 10: Workflow for reference BEMT computations

The simplest method to consider this variation would be in accordance with a power law [23]. The stress range associated with the fluctuations would be comparatively low, but at high frequency. The stress ratio would be either purely tensile or purely compressive, depending on the ply under consideration. A proposed schematic for these computations, using a Blade Element Momentum Theory (BEMT) model, is shown in Figure 10. The blade is subjected to a spatially varying velocity field, at a constant TSR, for different inflow axial velocities. The BEMT model developed under Task 3.1 of the RealTide project [24] – 'StarBlades', is a tool which can be used to execute this task.

The BEMT computations, are performed for one full rotation of the blade, and for each inflow velocity, a sinusoidally varying root bending moment on the blade is obtained, as can be seen from the figure. A parabolic fit would describe a transfer function between the inflow velocity and the maximum root bending moment. Given a tidal velocity spectrum (which is characteristic of the site), this transfer function can be used to convert it into an equivalent bending moment spectrum. Subsequently, the ply-by-ply approach can be used to transfer it into a stress spectrum.

Waves: The characterisation of fluctuations due to waves is to be done stochastically. For marine applications such as for ships in service, the most commonly used probability distribution function to define the encounter waves is the Weibull distribution function [25]. This function is defined by a shape parameter and a characteristic value. The shape parameter is usually defined in the Class rules. The characteristic value is provided by the response of the ship to a characteristic wave corresponding to 10^{-2} probability of occurrence. An application of the Weibull probability distribution for a composite-hull vessel has been provided in [26]. A similar approach can be used to define the wave spectrum of loads on the tidal blades.

Turbulence: Turbulent fluctuations in the inflow velocity causes very high frequency stress fluctuations on the blade. The representation of these fluctuations can be characterised by Computational Fluid Dynamics (CFD) simulations. For wind turbines operating in complex terrain, it is observed that the main driving fatigue mechanism is the turbulence intensity [27]. The characterization by means of CFD is however computationally intensive.

3.4.2 Stress Spectra

Section 3.4.1 describes the various sources of force fluctuations in a tidal turbine operating environment. When these are accounted for, the result would be in the form a force or bending moment spectra on the entire blade. The next step would be to transform this into equivalent stress spectra, so that the fatigue assessment methodology can be implemented. Figure 11 shows a workflow for this conversion using a BV freeware tool - ComposeIT [15]. ComposeIT tool is based on composite macro-mechanics, and it enables the ply-by-ply stresses on a laminate with a given stacking sequence and applied load to be computed. In the case of a tidal turbine, the laminate loads can be either computed using simple beam theory (see Figure 10) or using a Finite Element Analysis (FEA) model. Once the ply-by-ply stresses for one loading condition are determined, a linear transfer function can be used to convert the bending moment spectrum into a stress spectrum – assuming that the deformation of the blade is linear and elastic. As fatigue damage is accumulated over a large number of cycles, the blade deformation is expected to be linear when subjected to these forces, and the linear elastic assumption is very relevant.

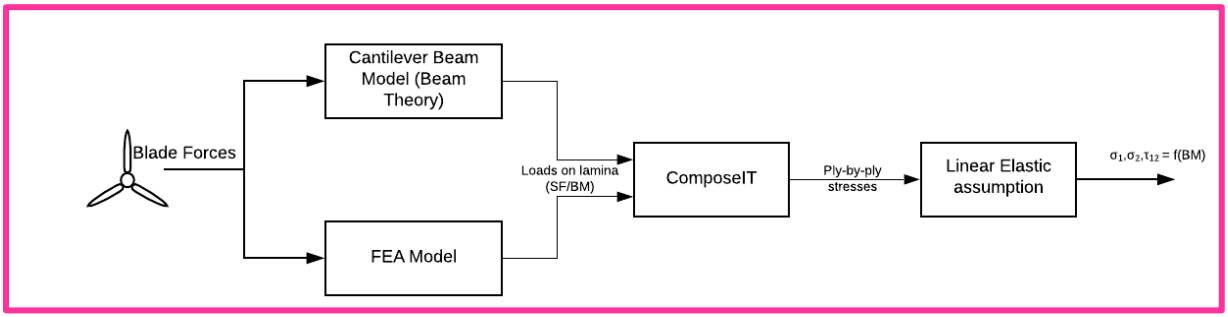

Figure 11: Workflow for reference stress calculations using ComposeIT

3.5 EXTRAPOLATION OF S-N CURVE DATA FOR MULTIPLE STRESS RATIOS

For elasto-plastic materials like steel, many practical applications consider the same S-N behaviour for different stress ratios ($R = \sigma_{min}/\sigma_{max}$), at least for fully tensile cycles. However, the same is not true for visco-elastic materials like composite laminates; they have different S-N curve behaviour for different *R* ratios [28] [29]. In practical applications for fatigue design, such as for composite blades, it is very common that the loading histogram corresponds to cyclic stresses of multiple stress ratios.

For metals, the effect of varying stress ratio can be reasonably approximated by only considering the stress range of these cyclic stresses. This means that the fatigue behaviour for the entire loading history can be characterized by a single experimental campaign that determines the S-N curve for a suitably chosen *R* ratio. At the most, two different S-N curves are chosen to represent the tensile and compressive behaviours separately. On the contrary, if the fatigue behaviour for visco-elastic composite laminates need to be represented, this would require a testing campaign that includes fatigue testing for multiple R ratios. This would be a very time-consuming and impractical experimental testing campaign and would not be feasible in the various stages of design.

Within this section, various approaches are described that allow for the extrapolation of S-N curve data for one stress ratio, to another stress ratio. All these approaches are based on the Constant Life Diagrams (CLD), also known as Constant Fatigue Life (CFL) diagrams. The most commonly used form of CFL is the Goodman diagram [30] – a diagram which quantifies the interaction of mean and alternating stresses on the fatigue life of a material (see Figure 12 [31]). A typical CLD for wind turbine composite blade applications, extracted from [32], is shown as Figure 13. As can be seen, the effect of varying stress ratio on the fatigue life is significant, and needs to be adequately characterized within any fatigue prediction methodology for composite applications.

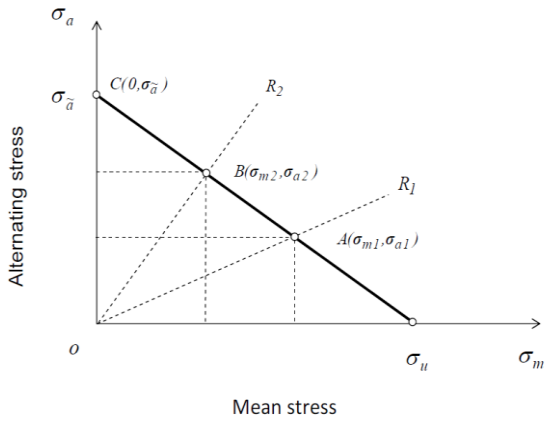

Figure 12: Goodman constant fatigue life diagram

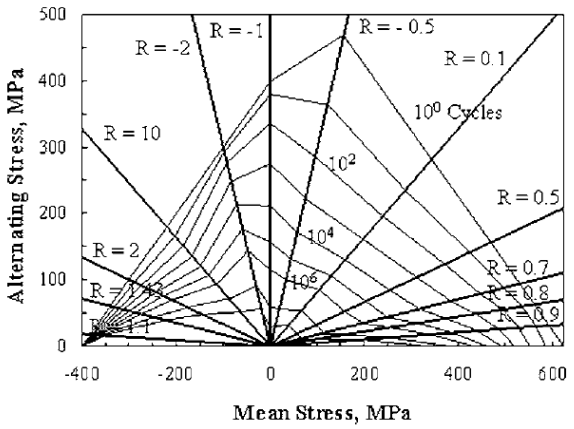

Figure 13: Typical CLD for wind turbine applications

Existing literature provides many techniques that allow for extrapolation of S-N curve data across different *R* ratios. A good compilation of most of the techniques is available in [33]. Most of the techniques mentioned, however, require experimental characterization with tests from multiple stress ratios and/or experimental curve fitting to obtain equation constants. In line with the objective of the global fatigue analysis methodology, the most suitable method would be linear extrapolation methods – as they do not require any curve fitting, and can be done with available test results. The accuracy of the linear extrapolation method is questionable; however, it generally provides conservative predictions.

3.5.1 Linear Extrapolation

The linear extrapolation method is based on the Goodman constant fatigue life diagram. Any point on the diagram corresponds to the same number of cycles of fatigue stresses, for example points *A* and *B* from Figure 12. Each point also corresponds to a particular stress ratio – a line joining the point to the origin of the graph would include all points at the particular stress ratio.

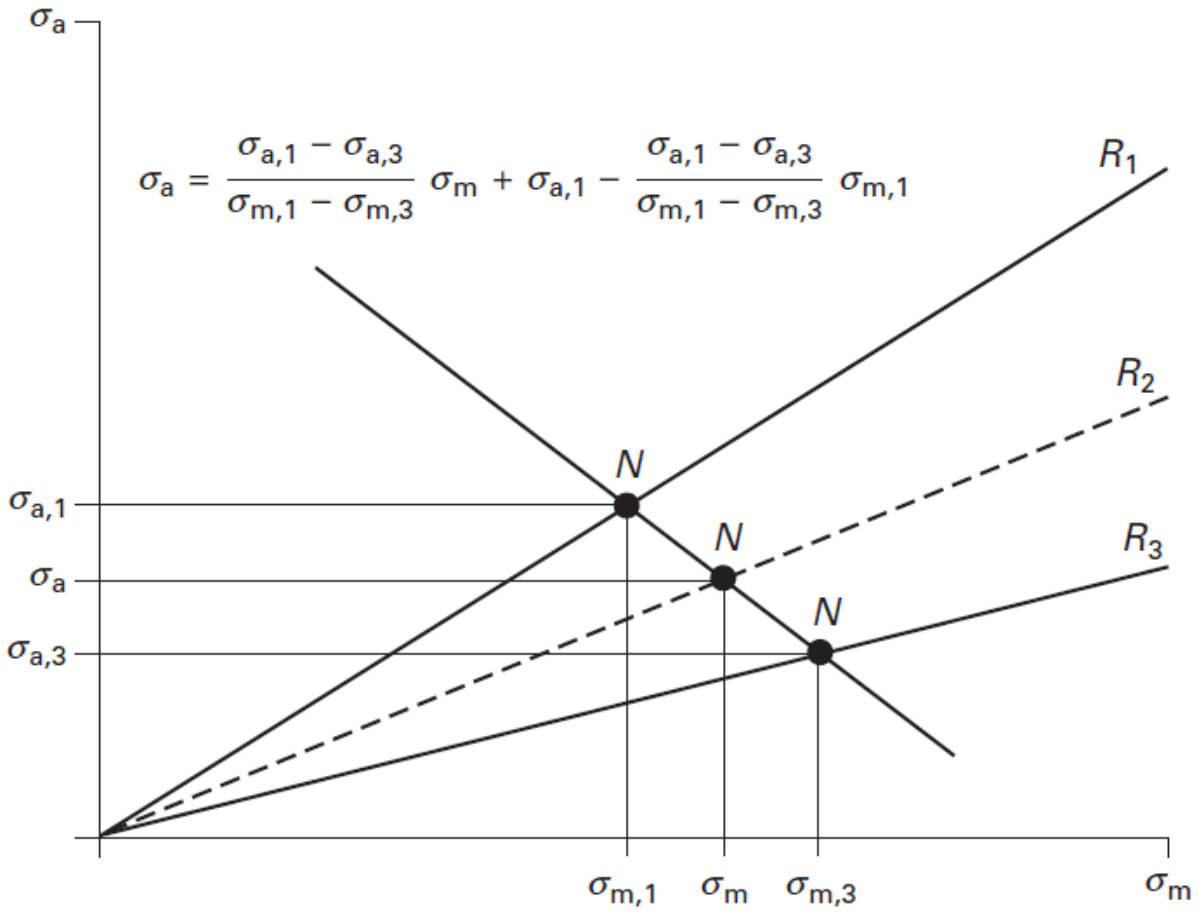

Figure 14: Illustration of the linear extrapolation method [34]

An illustrative example of the linear extrapolation method is extracted from [34] and shown as Figure 14. Knowing the values at two stress ratios (R_1 and R_3 respectively), the mean stress and stress amplitude corresponding to the same number of cycles (same fatigue damage state) for an intermediate ratio R_2 can be obtained by linear extrapolation. The stress amplitude (σ_a) for the intermediate ratio, can be derived as:

$$\sigma_a = \frac{\sigma_{a_1}(\rho_1 - \rho_3)}{(\rho_1 - \rho)\frac{\sigma_{a_1}}{\sigma_{a_3}} + (\rho - \rho_3)} \quad \text{..... Eq. 7}$$

Where ρ_i is an alternate stress ratio, defined as the ratio of the stress amplitude to the mean stress.

$$\rho_i = \frac{\sigma_{mean}}{\sigma_{amp}} = \frac{1 + R_i}{1 - R_i} \quad \text{..... Eq. 8}$$

If the fatigue test results for multiple stress ratios are available, like in Figure 12, then the results for any intermediate ratio can be interpolated using piecewise linear extrapolation. It is evident that the

extrapolation needs to be done separately for tensile and compressive regiments, as these would be represented by different lines on the Goodman diagram.

However, in most application cases, the availability of results for multiple stress ratios cannot be guaranteed. Commonly, the results for one tensile stress ratio ($0 < R < 1$; $\rho > 1$) and one compressive ratio ($R < -1$; $\rho < -1$) would be available. Such a scenario is, essentially, an extended case of Equation 7, with R_3 being a point on the σ_m axis. For the tensile fatigue case, where σ_{UTS} is the ultimate tensile strength of the laminate, this would mean that:

$$R_3 = 1; \qquad \rho_3 = \infty; \qquad \sigma_{a_3} = 0; \qquad \sigma_{m_3} = \sigma_{UTS}$$

Equation 7 can thus be simplified as:

$$\sigma_a = \frac{\sigma_{UTS}}{\frac{\sigma_{UTS}}{\sigma_{a_1}} + \rho - \rho_1} \qquad \text{..... Eq. 9}$$

Similarly, for the compressive fatigue cases, where σ_{UCS} = Ultimate Compressive Strength of the laminate:

$$\sigma_a = \frac{\sigma_{UCS}}{\frac{\sigma_{UCS}}{\sigma_{a_1}} + \rho - \rho_1} \qquad \text{..... Eq. 10}$$

Equations 9 and 10 provide a linear extrapolation technique that allows extrapolation of fatigue results from one stress ratio to another. These analytical expressions are also present in the work by Vassilipoulos et al [35]. Similar extrapolation methods have been proposed by Westphal and Nijssen [4], wherein the expressions have been altered to obtain the number of cycles corresponding to any given stress amplitude and stress ratio. The solution for this case includes the slope parameter and intercept of the S-N curve, m_1 and k_1 respectively. The modified forms of Equations 9 and 10 are presented as Equations 11 and 12 respectively.

$$N = \left[\frac{k_1\left(\frac{\sigma_{UTS}}{\sigma_{a_1}} - \rho + \rho_1\right)}{\sigma_{UTS}}\right]^{m_1} \qquad \text{..... Eq. 11}$$

$$N = \left[\frac{k_1\left(\frac{\sigma_{UCS}}{\sigma_{a_1}} + \rho - \rho_1\right)}{\sigma_{UCS}}\right]^{m_1} \qquad \text{..... Eq. 12}$$

Although existing literature classifies the Goodman relation as conservative compared to experimental results, it still provides a reasonably good approximation; and the fact that the relation is linear, gives a relatively simple extrapolation method. This simplicity in application would provide a scientifically founded method to account for varying stress ratios in practical fatigue design problems. Given the experimental fatigue behaviour (S-N curve) of a composite laminate for a stress ratio, this technique is useful to approximately predict the fatigue behaviour of the same laminate for a whole new range of different stress ratios.

3.6 CHARACTERIZATION TESTS

One of the major objectives while formulating the methodology for fatigue analysis of composite laminates was to limit the number of tests required to experimentally characterise the fatigue behaviour. The methodology aims to characterise the fatigue behaviour of the uni-directional plies and then extend it to the application of any stacking sequence.

3.6.1 Required data

The main objective behind the analytical methodology is to perform a fatigue evaluation, with minimum data required from sample testing. For any given load state, the following material data is required to perform the computations using the proposed ply-by-ply fatigue analysis methodology. Table 3 provides a non-exhaustive list of tests that are required to be performed in order to use the ply-by-ply fatigue analysis methodology for the fatigue evaluation of composite laminates. An indicative list of standards that could be used for each test is also provided for information.

Table 3: Tests required for characterization of composite fatigue

Category	Properties	Standards
Elastic Properties	Elastic Modulus in L-direction (E_1) Elastic Modulus in T-direction (E_2) Shear Rigidity in L-T plane (G_{12}) Poisson ratio in L-T plane (v_{12} and v_{21})	ISO 3268
Ply properties	Fibre Volume Fraction Weight per unit area	Burn-off tests ISO 4605
Tensile Strength	Ultimate Tensile Strength in L-direction (S_{1T}) Ultimate Tensile Strength in T-direction (S_{2T})	ISO 527
Compressive Strength	Ultimate Compressive Strength in L-direction (S_{1C}) Ultimate Compressive Strength in T-direction (S_{2C})	ISO 604
Shear Strength	Ultimate In-Plane Shear Strength (S_{12})	
Fatigue of fibres	Tensile S-N curve for UD 0 degree ply (R=0.1) Compressive S-N curve for UD 0 degree ply (R=10)	ASTM D3479 ISO 14126
Fatigue of matrix	Tensile S-N curve for UD 90 degree ply (R=0.1) Compressive S-N curve for UD 90 degree ply (R=10)	ASTM D3479 ISO 14126
Residual Stiffness	(i) fatigue tests with continuous evaluation of stiffness using strain gauges/extensometers/DIC OR (ii) interrupted fatigue tests with stiffness measurements using low rate tensile loading tests	

According to rules, elastic properties and failure limits for the uni-directional are required to be experimentally obtained during the static strength evaluation of the laminate [14] [36]. Within Task 1.3 of the RealTide project, an experimental campaign was conducted to determine these properties for the composite materials used in tidal turbine blades [37] [38].

To characterize the fatigue behaviour, the minimum requirement is to have one S-N curve each describing the tensile and compressive fatigue behaviour. The stress ratios of R = 0.1 and R = 10 are chosen, as these are ratios that are typically used for experimental fatigue testing. The S-N curve for the UD 0 degree ply is presumed to represent the fatigue in the fibres; and the S-N curve for UD 90 degree ply is presumed to represent the fatigue of the matrix.

4 EXPERIMENTAL CAMPAIGN

4.1 EXPERIMENTAL SET-UP

4.1.1 Static tests

Tensile tests were performed according to ISO 527 on an Instron™ testing machine using a load cell of 200 kN at a crosshead speed of 2 mm/min. These were carried out on [0°], [90°], [0°/90°] and [0°/±45°] specimens. Strain was measured using a mechanical extensometer with a gauge length of 70 mm and modulus was calculated from the slope of the stress-strain plots over the strain range 0.05-0.25%. For each test sequence, 5 specimens were tested whose dimensions were 250 x 25 x 2 mm^3. All tests were performed using tapered [±45] glass/epoxy tabs at both specimen ends.

4.1.2 Fatigue tests

Tensile fatigue tests were performed on an MTS servo-hydraulic machine using a load cell of 250 kN at a frequency of 2 Hz. Most tests were performed at an R-Ratio of 0.1 and three tests were run at R=0.5. For all tests, hydraulic grips were used. For most specimens, fatigue tests were interrupted every decade to measure the change in modulus as a function of fatigue life. To do that the method described in 4.1.1. was used.

4.2 STATIC MECHANICAL PROPERTIES

Results from static tests performed on [0°], [90°], [0°/90°] and [0°/±45°] specimens are shown hereafter, Figure 15. The stresses at failure for each sequence are then summarized in Table 4.

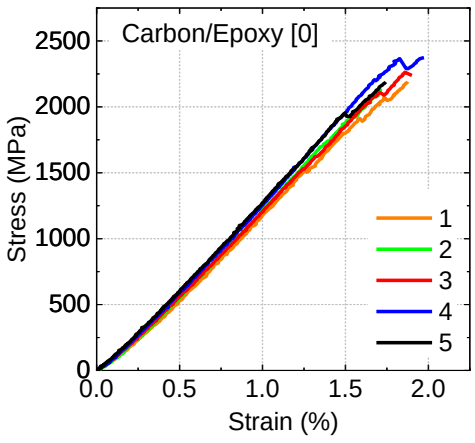

(a)

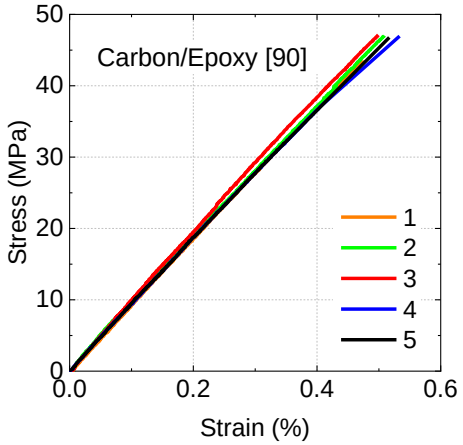

(b)

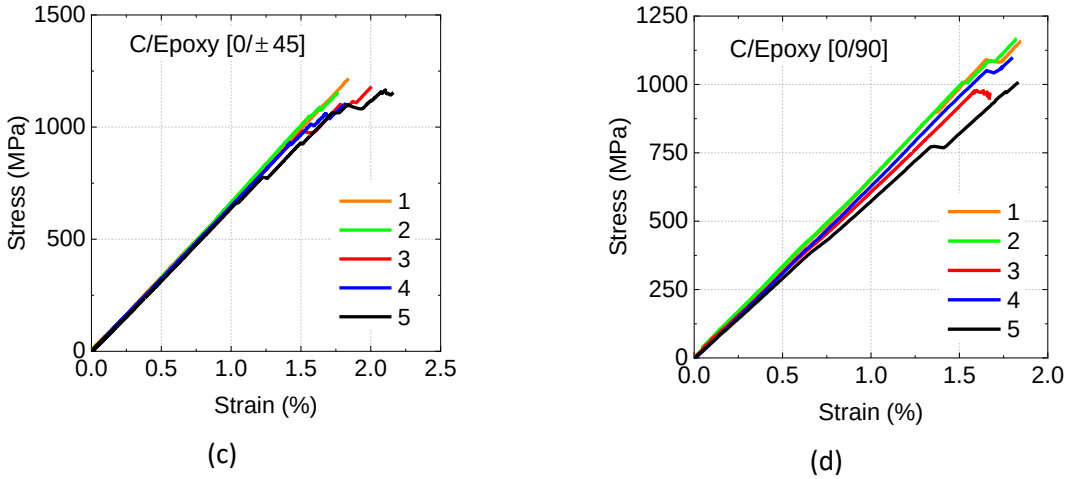

Figure 15: Stress-strain plots from static tensile tests for (a) [0] (b) [90] (c) [0/±45] (d) [0/90] specimens

Table 4: Stress at failure obtained from static tests

Sequence	Stress at failure (MPa)
[0°]	2285 ± 102
[90°]	45 ± 2
[0/±45°]	1164 ± 40
[0/90°]	1082 ± 86

4.3 S-N CURVES FOR UNIDIRECTIONAL SPECIMENS

Results concerning fatigue tests performed on unidirectional specimens are shown in Figure 16.a for [0°] specimens and in Figure 16.b for [90°] specimens. On each Figure, arrows are used to indicate data points correspond to runout tests.

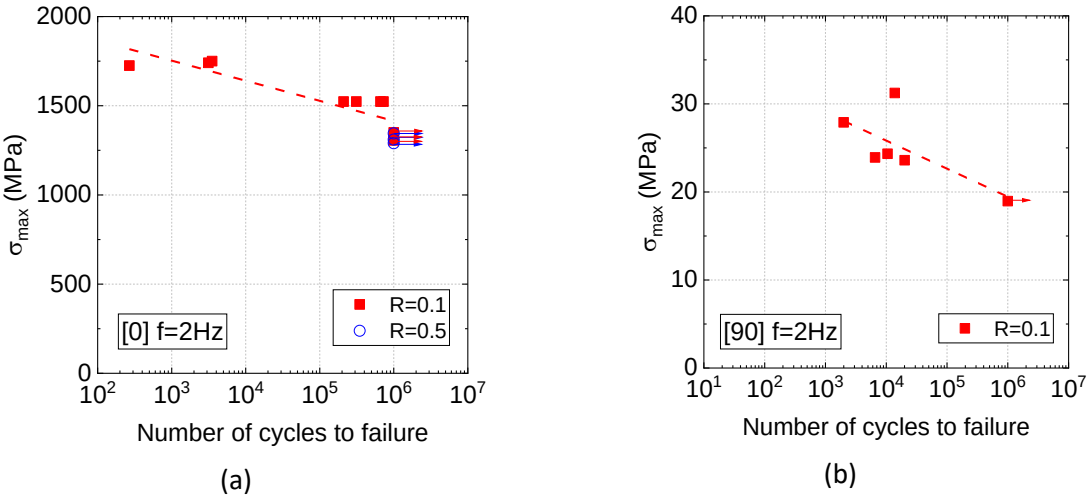

Figure 16: S-N curves for unidirectional specimens (a) [0] (b) [90]

Then fatigue test results concerning [0/90] and [0/±45] specimens are shown in Figure 17.a and Figure 17.b.

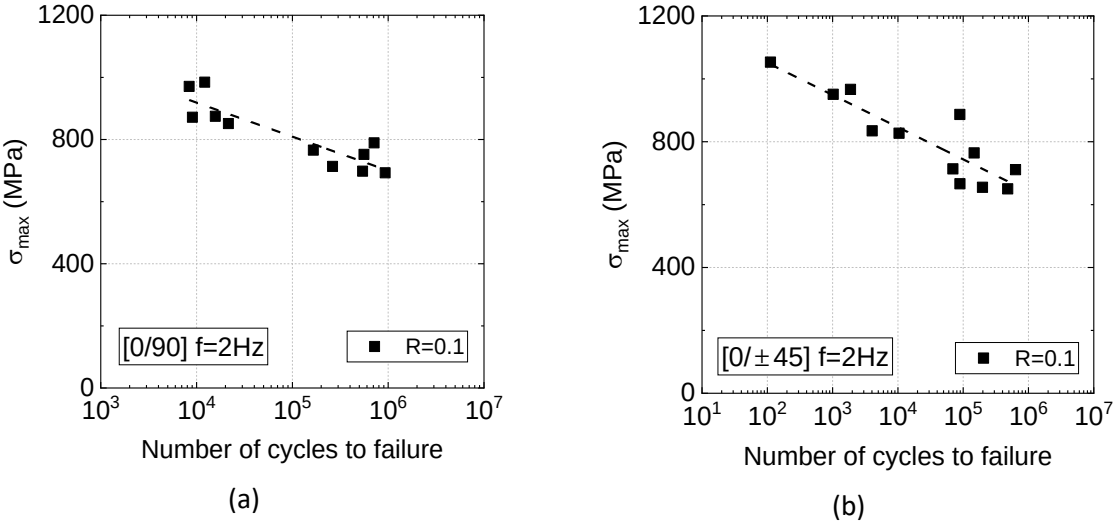

Figure 17: S-N curves for (a) [0/90] (b) [0/±45] specimens

4.4 STIFFNESS AND STRENGTH DEGRADATION DURING FATIGUE LIFE

4.4.1 Unidirectional specimens

First, interrupted fatigue tests were performed on unidirectional specimens loaded in the longitudinal direction. Changes in stiffness for specimens loaded at 80% of the static strength at an R-ratio of 0.1 are shown in Figure 18. Results show very little change in stiffness (around -2.5%). Such a result is expected because the behaviour is fibre dominated.

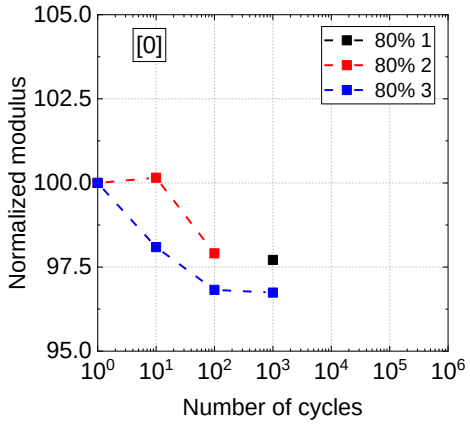

Figure 18: Change in stiffness as a function of number of cycles for unidirectional specimens loaded at 80% of static limit in the longitudinal direction

Then, the effect of R-ratio on the stiffness changes was investigated for a maximum load of 60%. Results for modulus changes at two different R-ratios (0.1 and 0.5) are presented in Figure 19 and show that no decrease in stiffness is observed.

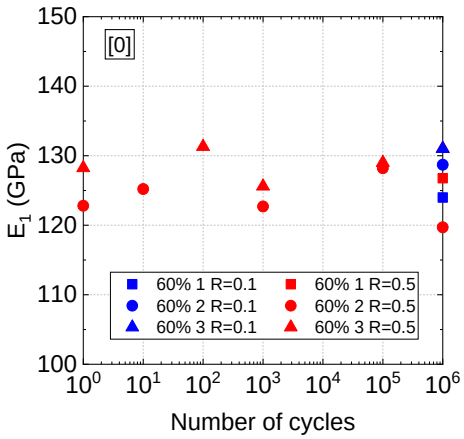

Figure 19: Change in longitudinal modulus as a function of number of cycles for unidirectional specimens loaded at 60% of static limit at R=0.1 and R=0.5

The specimens used to perform the fatigue tests that ran out to one million cycles at an R-ratio of 0.5 were then tested to investigate their static residual strength, Figure 20. Despite a higher scatter, results do not show significant degradation after one million cycles, which is in accordance with the fact that no change in modulus was observed in Figure 19.

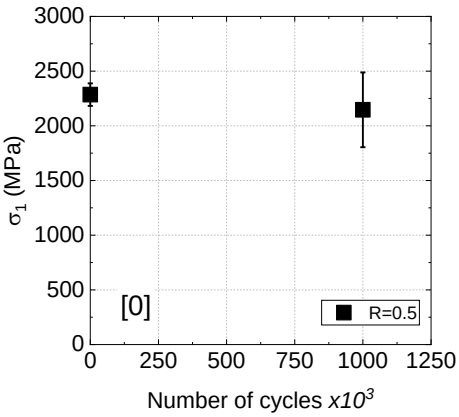

Figure 20: Residual strength of unidirectional specimens loaded up to one million cycles at R=0.5 at 60% of static strength

Similar tests were performed on unidirectional specimens loaded in the transverse direction. Changes in stiffness are shown in Figure 21 (from fatigue tests performed at 40% of static strength). These show no decrease in modulus, which may be associated with the fact that the test was performed at quite a low percentage of the static strength. It may be noted that performing interrupted tests on [90] specimens is not easy because specimens are very sensitive to experimental handling.

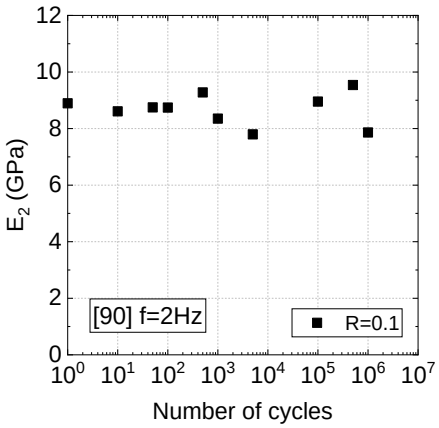

Figure 21: Change in transverse modulus as a function of number of cycles for an unidirectional specimen loaded at 40% of static strength

4.4.2 [0/90] and [0±45] specimens

The stiffness degradation is investigated in this section for different stacking sequences. First on the [0/90] sequence (Figure 22) and then on the [0/±45] sequence (Figure 23). For the [0/90] stacking sequence, there is a decrease in stiffness of approximately 15% before failure while the decrease for the [0/±45] stacking sequence is around 5 to 10%.

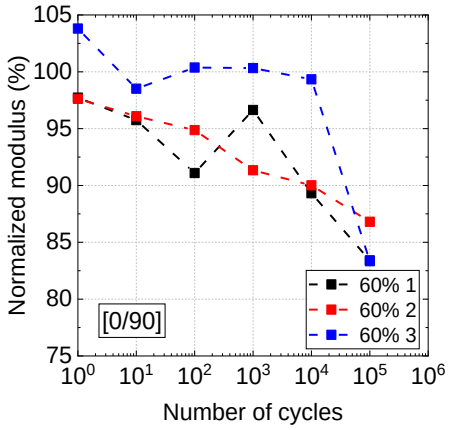

(a)

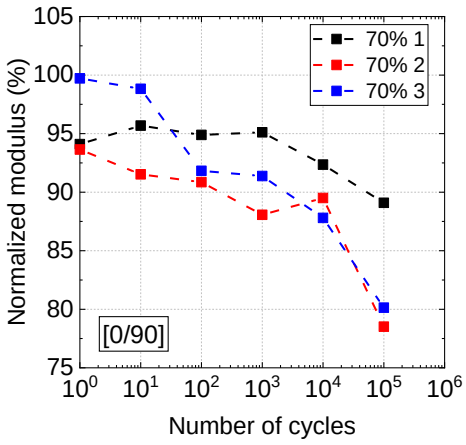

(b)

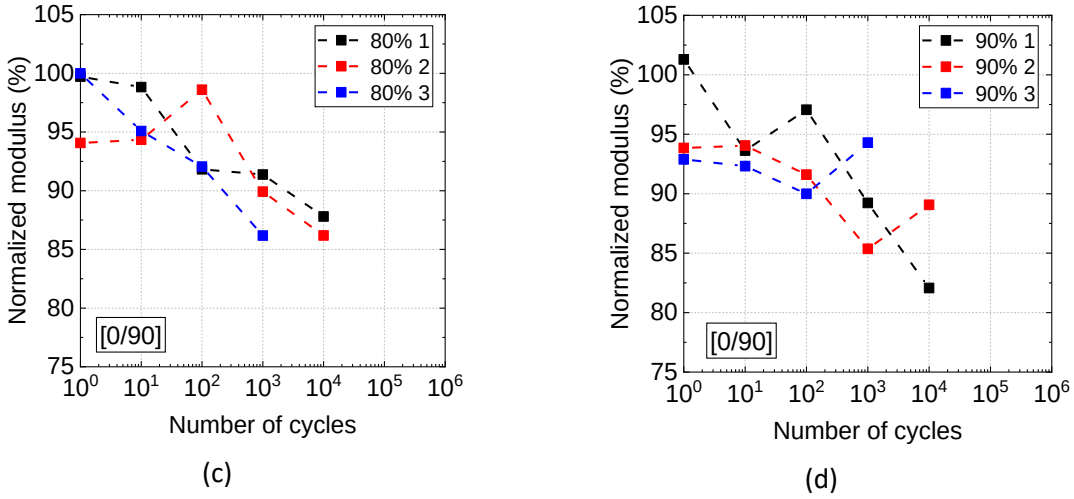

Figure 22: Change in stiffness as a function of number of cycles for [0/90] specimens

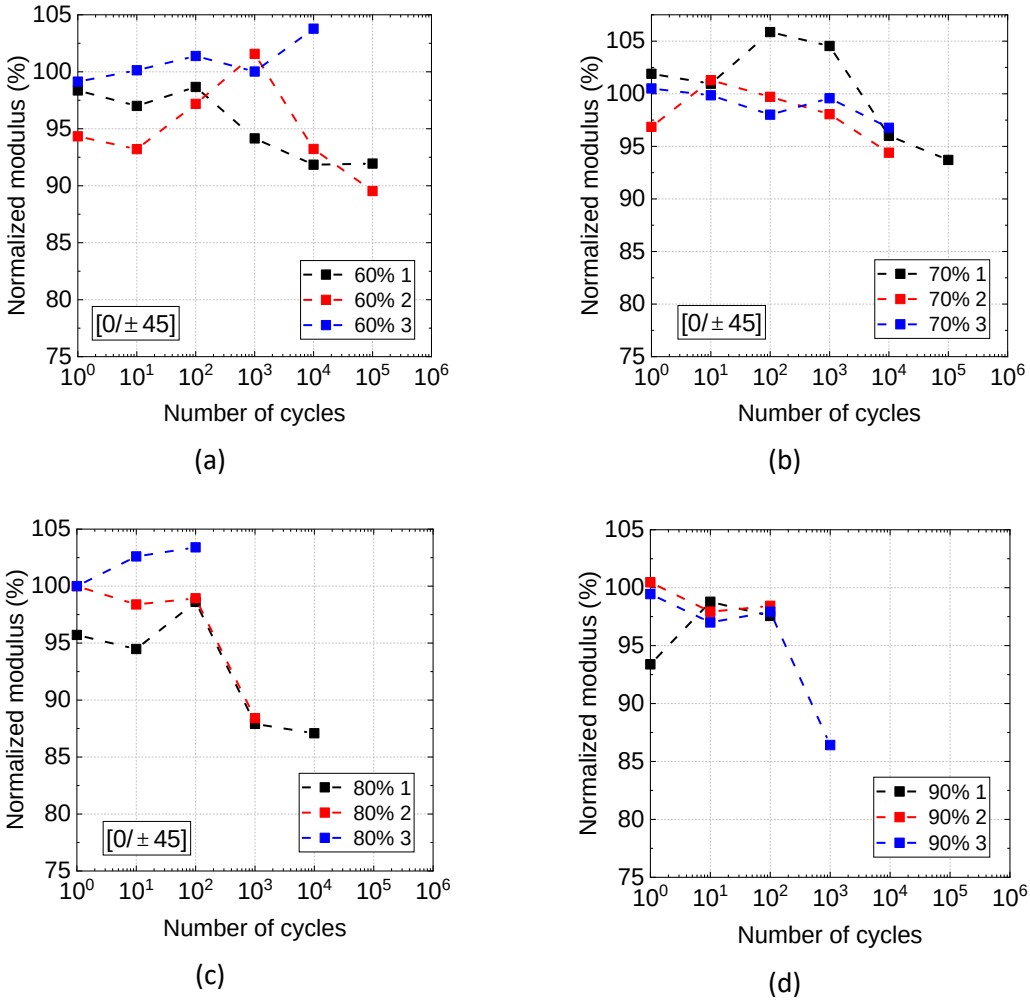

Figure 23: Change in stiffness as a function of number of cycles for [0/±45] specimens

5 VALIDATION CASE STUDIES

It is necessary to perform validation studies to confirm the suitability of the proposed fatigue methodology to applications related to tidal turbine blades. However, with the loads on a tidal turbine blade being highly complex to measure in real sea conditions, such validation data are not readily available. Hence, it is impractical to perform a validation of the entire global fatigue methodology at this stage. It is expected that the deployment of Sabella D10 turbine, as a milestone achievement of the RealTide project, will contribute to bridging this gap.

The proposed global fatigue methodology is a combination of different hypotheses, as explained in the various sub-sections of Section 3. As a starting point, it would be appropriate to do the validation of each of these suppositions, as these are not conclusively proved in the literature for existing industrial and/or research applications. The focus within this deliverable is to establish the validation of the various sub-scale approaches that make up the proposed global fatigue analysis methodology.

5.1 VALIDATION OF PLY-BY-PLY APPROACH FOR FATIGUE

The ply-by-ply approach towards fatigue, explained in Section 3.1, provides a simplified approach for fatigue analysis, by computing equivalent fibre and matrix stresses. The approach is a shift from the classical method of characterizing the fatigue behaviour of the entire laminate, towards an approach that is more micro-mechanical. As there are multiple failure mechanisms in action during the fatigue of a composite laminate, the validation of this approach is necessary to give an overview about its applicability and limitations.

An interesting database that could be used to test the applicability of this method, was obtained from the work of Kawai et al [39]. The Kawai experiments [39] provide a database for fatigue testing of off-axis laminates. From a laminate stacked with 16 unidirectional plies at 0°, samples were cut at different angles – 0°, 10°, 15°, 30°, 45° and 90°. Static failure limits for these were obtained through tensile and compressive tests (see Table 5).

Table 5: Tensile and Compressive strength of off-axis UD T700S/2592 carbon/epoxy laminate

Angle, θ (°)	$\sigma_{Tension}$ (MPa)	$\sigma_{Compression}$ (MPa)
0	1887.1	-806.5
10	343.0	-313.0
15	210.9	-234.0
30	101.1	-163.6
45	61.6	-151.6
90	30.1	-154.0

Table 6: Macroscopic fatigue failure modes observed for different loading conditions [39]

	R							
θ (°)	0.5	0.1	χ	−1	−3	−10	10	2
0	T	T	T, C_K, C_{IS}	C_K, C_{IS}	–	–	C_K, C_{IS}	C_K, C_{IS}
10	T	T	T, C_K, C_{IS}	–	C_K, C_{IS}	–	C_K, C_{IS}	C_K
15	T	T	T, C_K, C_{IS}	–	C_K, C_{IS}	–	C_K	C_K
30	T	T	T, C_{IS}	–	T, C_K, C_{IS}	–	C_K	C_{IS}, C_{OS}
45	T	T	T	T	–	T, C_{OS}	C_{OS}	C_{OS}
90	T	T	T	T	–	T, C_{OS}	C_{OS}	C_{OS}

T: tensile failure; C: compressive failure; C_K: kink failure; C_{IS}: in-plane shear failure; C_{OS}: out-of-plane shear failure; –: NA

Thereafter, fatigue tests on each of the samples were performed, for multiple R ratios. The S-N graphs for all these tests are provided; and also the macroscopic fatigue failure modes observed for different loading conditions, as can be seen from Table 6.

5.1.1 Validation Approach

The data available from the research paper is used to validate the fatigue evaluation procedure using UD S-N curves, explained in Section 3.3.1. For the various off-axis plies (10°, 15°, 30° and 45°), the fatigue S-N curve is predicted with the proposed methodology, using the data from the UD 0° and UD 90° S-N curves. The static failure limits for the laminate are estimated from the available static test results (Table 5). These are summarized in Table 7 below.

Table 7 : Static failure limits for UD ply

Item	Description	Value
S_1 (Tension)	Ultimate Failure Strength (Tension) in L-Direction	1887 MPa
S_1 (Compression)	Ultimate Failure Strength (Compression) in L-Direction	-806.5 MPa
S_2 (Tension)	Ultimate Failure Strength (Tension) in T-Direction	30.1 MPa
S_2 (Compression)	Ultimate Failure Strength (Compression) in T-Direction	-154.0 MPa
S_{12}	Ultimate Shear Failure Strength in L-T plane	±75.8 MPa

The validation is performed for multiple stress ratios: R = 0.1 for tension-tension fatigue and for R = 10 for compression-compression fatigue. These ratios are chosen, since the test data is available for all the orientation angles (see Table 6). It is to be noted that the laminates used for these experiments are unbalanced off-axis plies. Hence, the formation of a matrix crack is likely to lead to a fatal propagation that results in the failure of the entire laminate. Therefore, the failure of the matrix (using the UD 90° S-N curves) is taken as the point at which the laminate is predicted to fail. The results from the simulation are presented in the subsequent section.

5.1.2 Results for fatigue of off-axis plies in tension

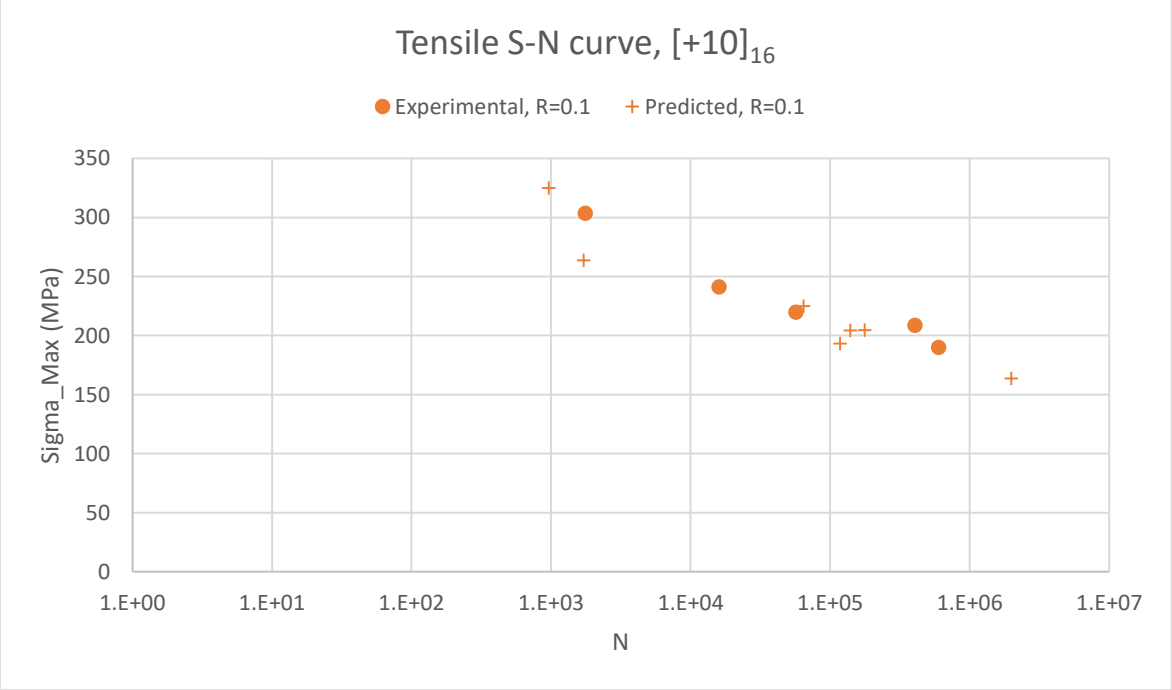

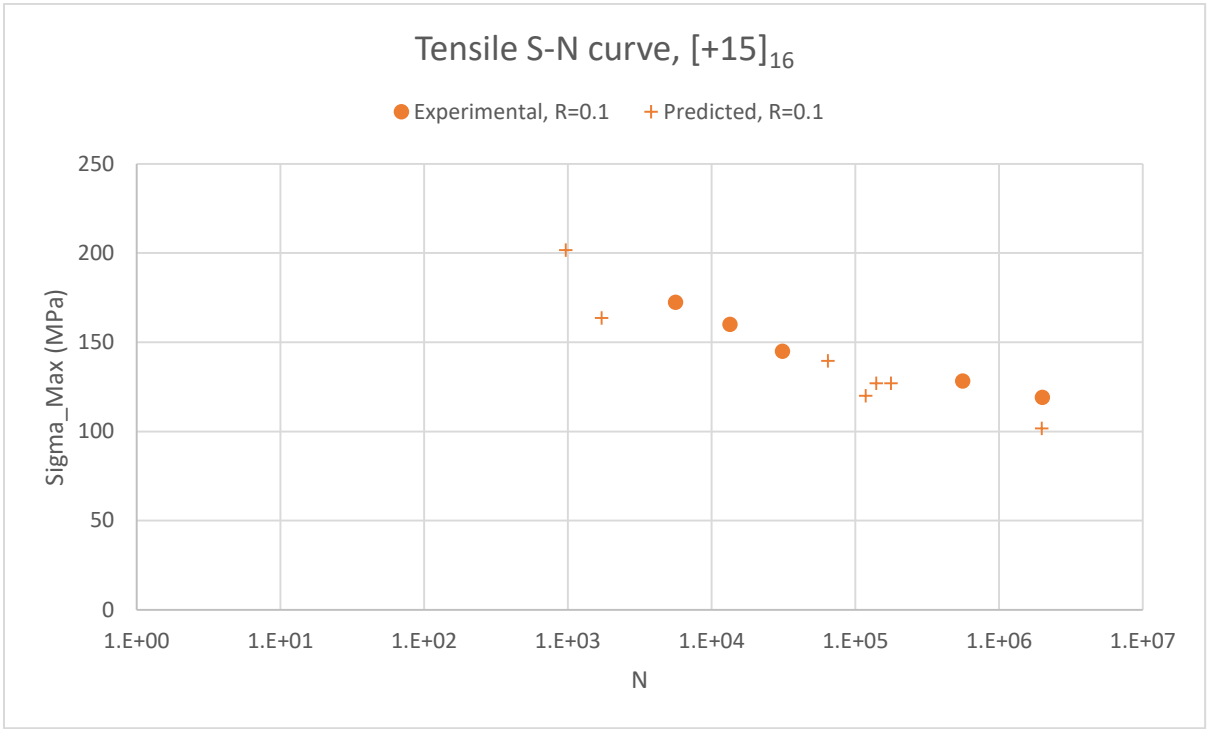
Tensile S-N curve, [+15]16
Experimental, R=0.1
Predicted, R=0.1
Sigma_Max (MPa)
250
200
150
100
50
0
1.E+00
1.E+01
1.E+02
1.E+03
1.E+04
1.E+05
1.E+06
1.E+07
N

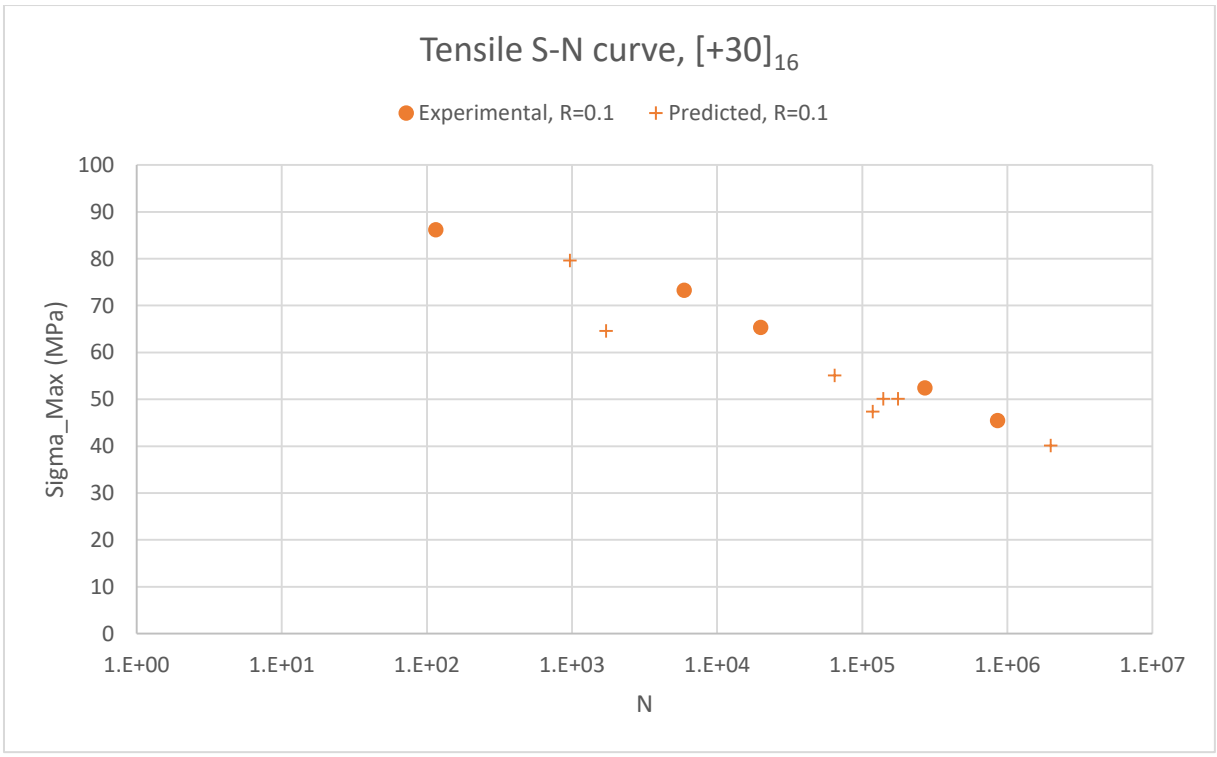
Tensile S-N curve, [+30]16
Experimental, R=0.1
Predicted, R=0.1
Sigma_Max (MPa)
100
90
80
70
60
50
40
30
20
10
0
1.E+00
1.E+01
1.E+02
1.E+03
1.E+04
1.E+05
1.E+06
1.E+07
N

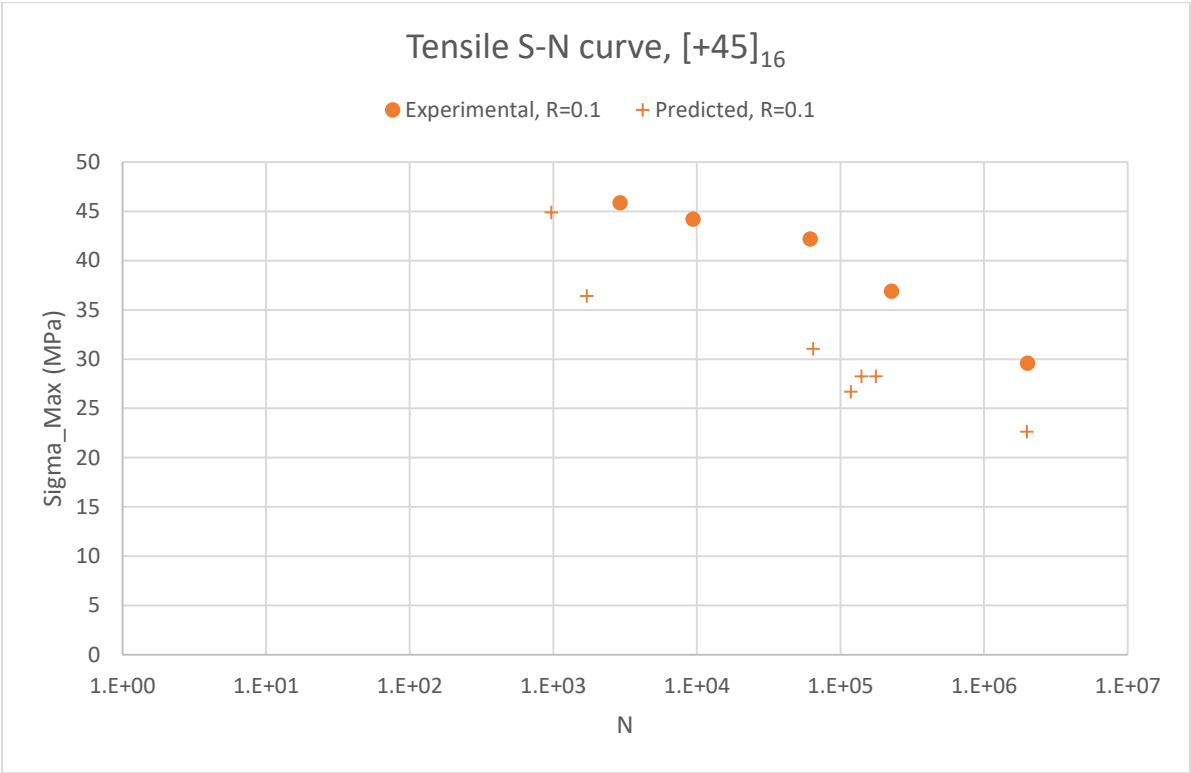

5.1.3 Results for fatigue of off-axis plies in compression

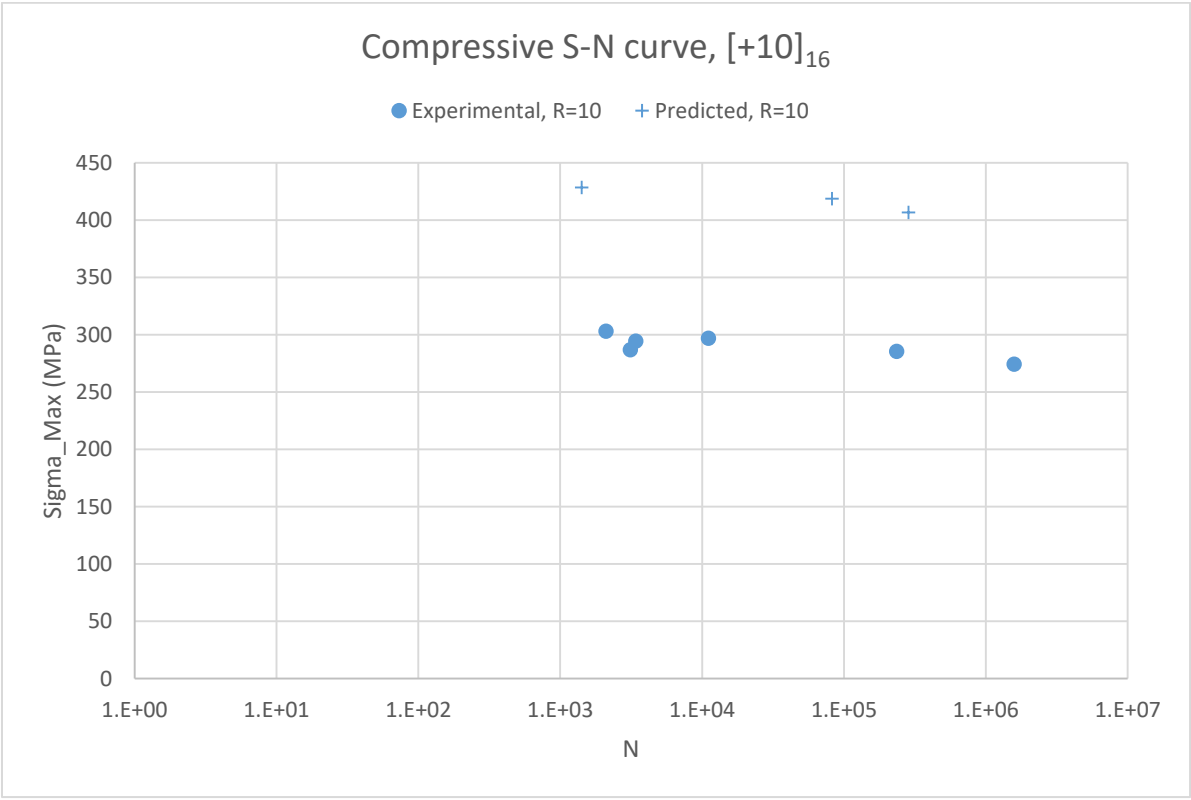

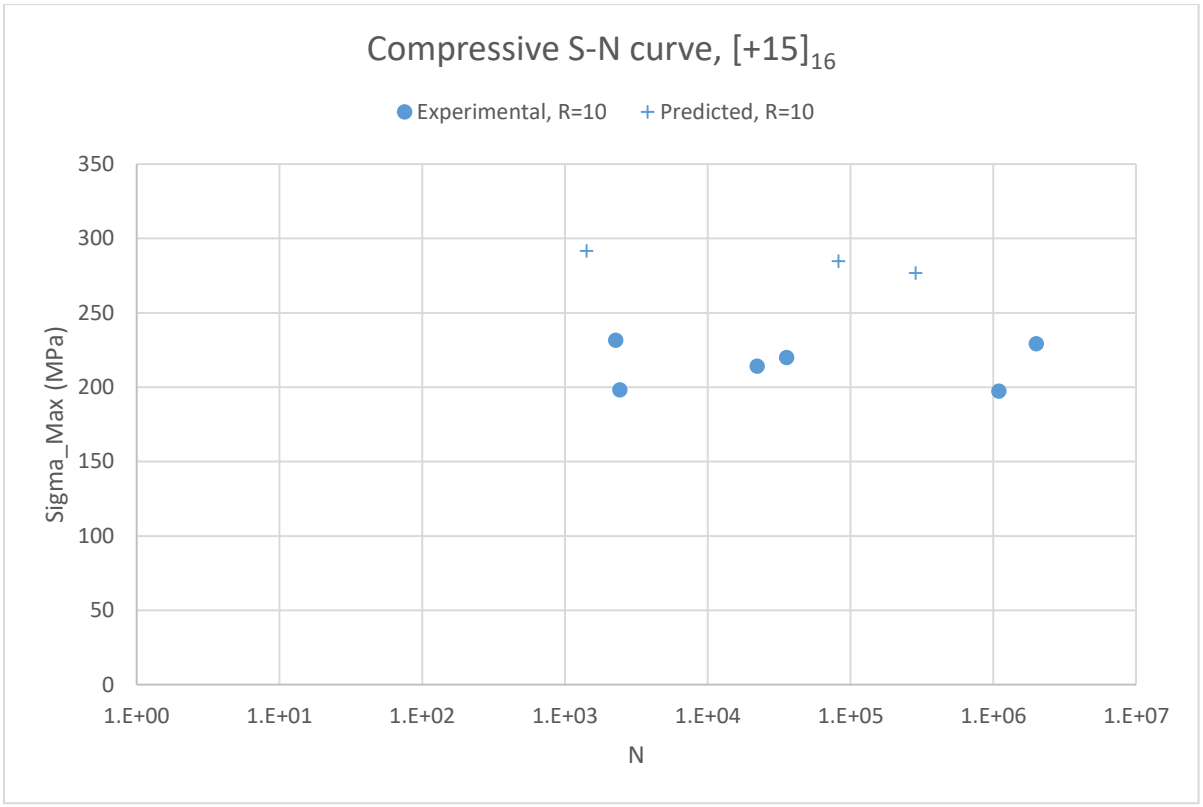
Compressive S-N curve, [+15]16
Experimental, R=10
Predicted, R=10
Sigma_Max (MPa)
350
300
250
200
150
100
50
0
1.E+00
1.E+01
1.E+02
1.E+03
1.E+04
1.E+05
1.E+06
1.E+07
N

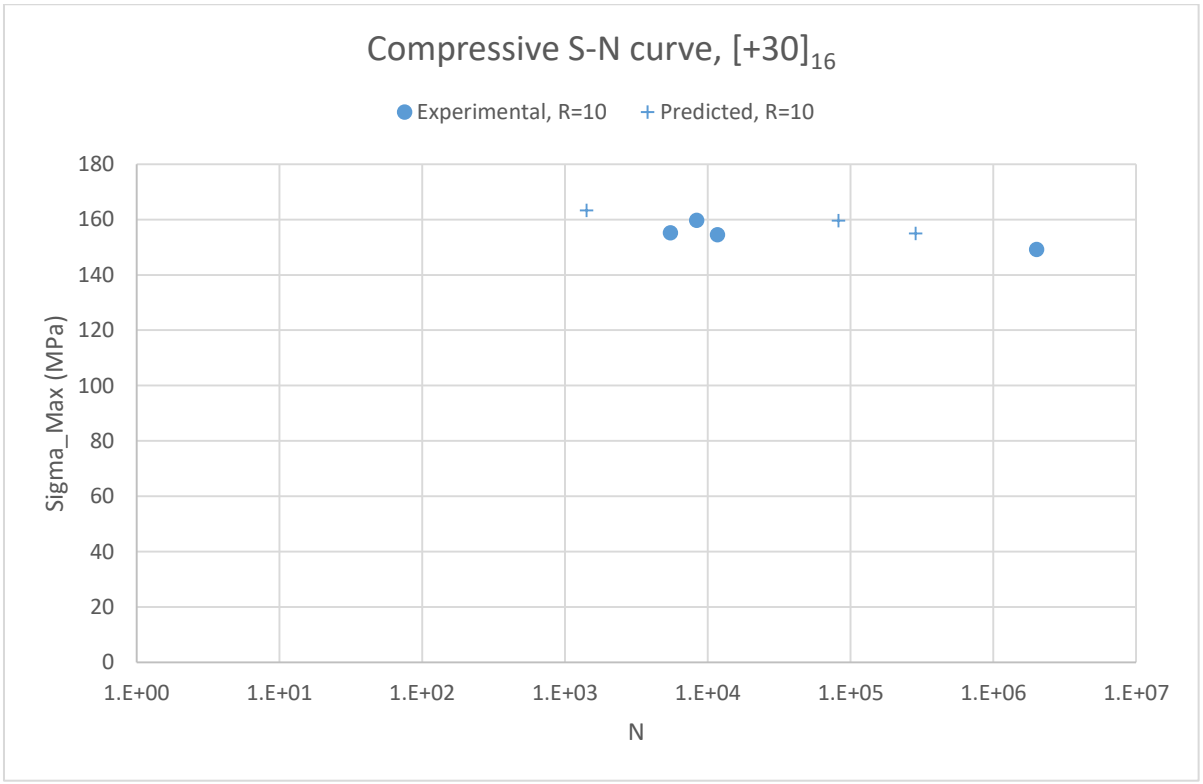
Compressive S-N curve, [+30]16
Experimental, R=10
Predicted, R=10
Sigma_Max (MPa)
180
160
140
120
100
80
60
40
20
0
1.E+00
1.E+01
1.E+02
1.E+03
1.E+04
1.E+05
1.E+06
1.E+07
N

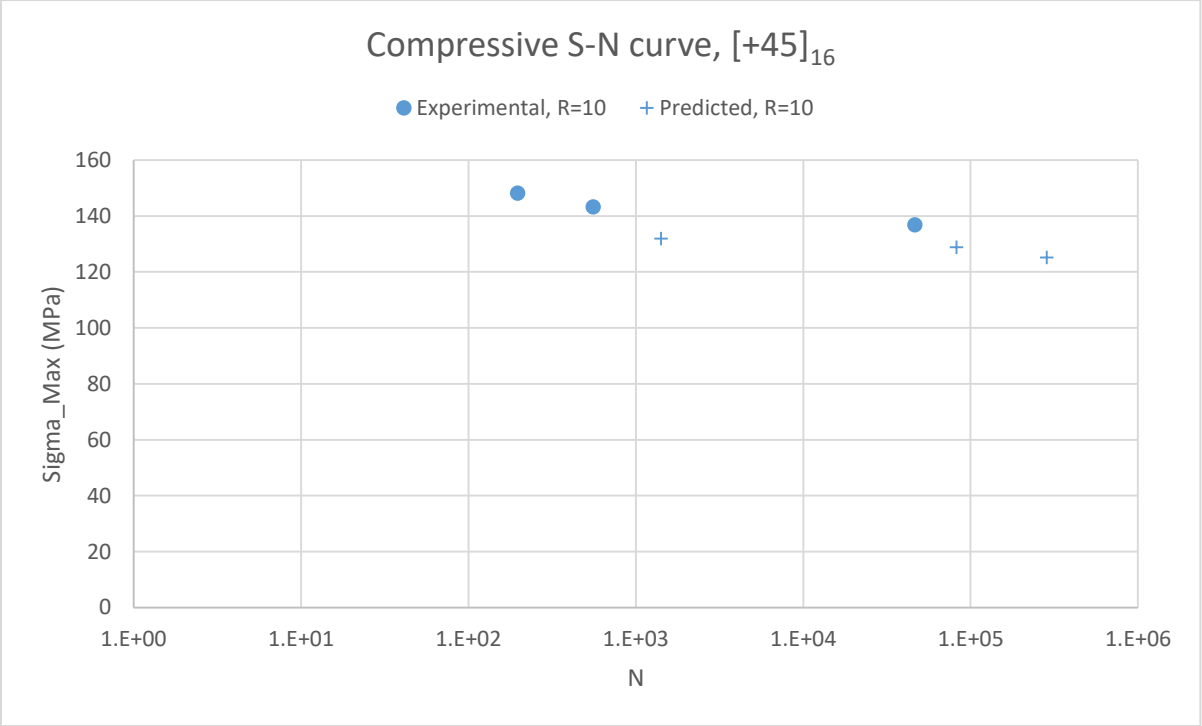

5.1.4 Discussion of Results

For the tensile fatigue S-N curves, the methodology shows very good correlation for all the ply orientation (+10°, +15°, +30°, +45°). The only exception is in the case of +45° for R=0.1, wherein the methodology is more conservative in predicting the fatigue life. The mechanism for failure for all the cases seems to be the same (tensile failure) from Table 6. A possible reason could be that for the +45° samples, the elliptic approximation of the equivalent matrix stress is quite conservative. This can be seen by referring back to Figure 5, wherein the actual failure envelopes from experimental tests are shown. For the +45° samples, the ratio σ_y:τ_{xy} is such that it falls almost along the diagonal, and for such a stress state, an elliptical formulation is clearly conservative. Further light on this can be shed from validation with other test data, for [45°] or [±45°] samples.

For the compressive fatigue, the methodology seems to be in good agreement for [+30°] and [+45°] laminates, but it seems to be over-estimating the fatigue life for [+10°] and [+15°] laminates. This might be due to the fact that for the [+10°] and [+15°] laminates, the stress in the L-direction (σ_1) is much higher than that for the other two laminates. This high compressive stress along the fibre direction can lead to premature micro-buckling of the fibres, which might supersede the matrix cracking fatigue. A hint of this can also be seen from the macroscopic fatigue failure modes in Table 6. For [+10°] and [+15°] laminates at R=10, one of the modes of failure is the kink failure – this mode of failure is related to micro-buckling. This mode of failure becomes less significant as the fibre orientation angle increases.

The equivalent matrix stress methodology evaluates compressive fatigue behavior based on the behavior of the [90°] laminates – which fails in out-of-plane shear. This can be extended to plies in [+30°] and [+45°] laminates, but it might be over-estimating the fatigue life of lesser orientation angles. However, in reality, the stacking sequence would be balanced, and such micro-buckling would be prevented. Hence, this methodology is expected to have better agreement for balanced plies subjected to a compressive load.

5.2 VALIDATION OF RESIDUAL STIFFNESS FORMULATION

In Section 3.2, an approach is explained which intends to augment the stress experienced by the fibres in terms of the progressive degradation of the stiffness of the laminate. A survey of the existing literature uncovered many such approaches that define the stiffness degradation of the laminate [40]. However, most of these represented the stiffness degradation as a function of the crack spacing or crack density, and hence were difficult to implement within the proposed global fatigue methodology.

The method proposed by Ogin et al [22] describes an equation which characterizes stiffness degradation as a function of the number of cycles. Such a method was found suitable and relatively easy to implement within the proposed framework. The equation used to describe the augmented stress in Section 3.2 is derived from the results of this research paper.

During the experimental campaign at IFREMER as part of the RealTide Task 1.4 (explained in Section 4), fatigue tests were conducted on combined laminates ($[0/90°]_{2s}$ and $[0/\pm45°]_{2s}$) with interrupted stiffness measurements of the laminate at various stages. The stiffness degradation during fatigue life was measured and plotted in Section 4.4.2. Within this validation study, a curve-fit of Equation 4 to this stiffness degradation is attempted, and the results are presented in this section. As a reminder, Equation 4 describes the stiffness degradation as a function of number of cycles:

$$E(N) = E_0 * \left[1 - \left(\frac{A}{k}\right)^k \left(\frac{\sigma_{max}^2}{E_0^2}\right)^{1-k} N^k\right]$$

Rearranging, we get $\log\left(1 - \frac{E(N)}{E_0}\right) = k \log N + \left[k(\log A - \log k) + 2(1-k)\log\left(\frac{\sigma_{max}}{E_0}\right)\right]$

Plotting $\log\left(1 - \frac{E(N)}{E_0}\right)$ vs $\log N$, enables the two constants A and k to be calculated.

5.2.1 Results

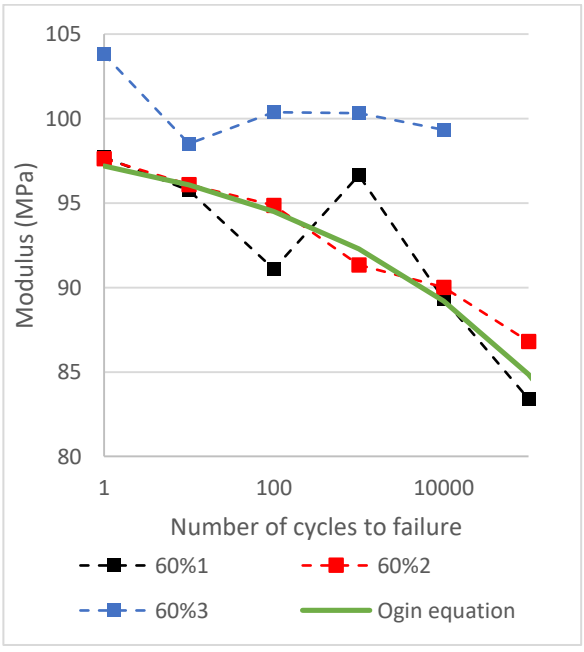

Figure 24: Curve-fit for stiffness degradation of $[0/90]_{2s}$ specimens

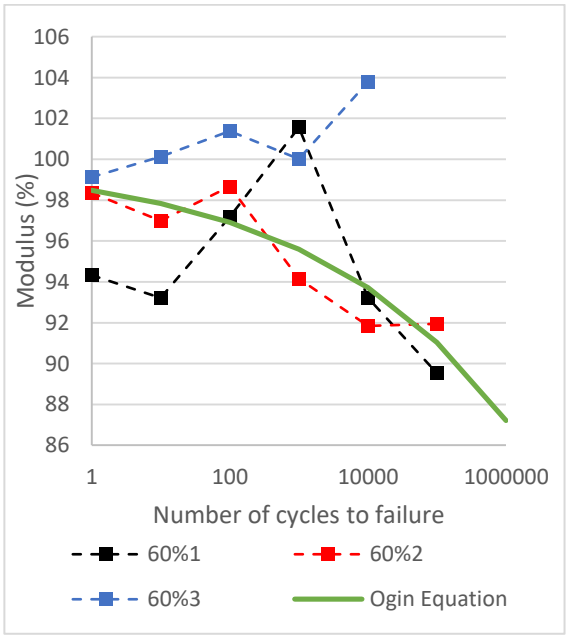

Figure 25: Curve-fit for stiffness degradation of $[0/\pm45]_{2s}$ specimens

In Figure 24 and Figure 25, the curve-fits for the stiffness degradation are shown for 60% fatigue loading. For higher loads, the final failure occurs relatively early, and hence there are not sufficient data points to do the curve-fit. The value of the curve-fit constants used are as follows:

For $[0/90]_{2s}$: A = 2.47E+11, k = 0.147
For $[0/\pm45]_{2s}$: A = 4.78E+09, k = 0.043

It was found that the values of the constants are very sensitive to the dispersion in the experimental data. This is mainly because these constants are obtained from the slope of the log-log graph. Due to this sensitivity, the constants used to plot the curve in Figure 24 and Figure 25 are obtained by choosing the best-fit value among the three readings, and not by averaging the results.

5.2.2 Discussion

From the results, it is evident that the stiffness degradation can be represented by a single function in terms of two experimental constants, as proposed by Ogin et al [22]. However, the determination of these constants is not straight-forward, and is very sensitive to the dispersion in the experimental data. Therefore, it cannot be established as a definitive formulation to characterize the stiffness degradation.

It must also be mentioned that within the experimental campaign, the stiffness was measured only at every decade, by interrupting the fatigue test and measuring the stiffness through low-strain loading. The accuracy of such curve-fit techniques depends on the number of data points available, and the usage of only a few data points could be one of the reasons for the sensitivity of the experimental constants. To verify this hypothesis, it is necessary to have continuous measurement of the stiffness of the sample using strain gauges or extensometers placed on the sample. Unfortunately, due to time and resource limitations, such measurements could not be made during this campaign.

Nevertheless, this validation study provides a promising step forward to characterize the stiffness degradation as a simple function. Once such a function can be determined for the laminate, it can be directly implemented in Equation 5 to account for augmented fibre stresses. Within the framework of the global fatigue analysis methodology, the residual stiffness formulation is proposed as a method to account for augmented fibre stresses. This formulation can be replaced by any suitable or more accurate equation, and can be directly integrated into the global framework. The lack of existing literature data regarding the degradation of stiffness as a function of number of cycles provides a hindrance for validating any residual stiffness formulation. To this end, it would be beneficial to continue experimental campaigns that continuously monitor the stiffness degradation of the samples during fatigue tests.

5.3 VALIDATING S-N CURVE EXTRAPOLATION FOR MULTIPLE STRESS RATIOS

One of the major difficulties in experimentally characterizing the fatigue behaviour of composite laminates is to extrapolate the results from one stress ratio to another. To overcome this difficulty, it has been proposed in Section 3.5 to make use of linear extrapolation using Goodman diagram approximation. Within the validation case study presented in this section, an application of the extrapolation technique has been performed based on the data available from the OPTIMAT project [41]. The OPTIMAT project comprised of a large scale testing campaign for composite laminates, generating a large database of static and fatigue experimental results. The project was performed in the context of wind turbine blades.

5.3.1 Validation Approach

From the OPTIMAT database, the S-N curves for three different stress ratios are extracted and plotted in Figure 26. The results are compiled for the same specimen type, laminates with stacking sequence $[[\pm 45, 0°]_4;\pm 45]$. The figure shows the variation of the fatigue behaviour for the same material, and hence also highlights the importance of considering the influence of stress ratio for composite laminates.

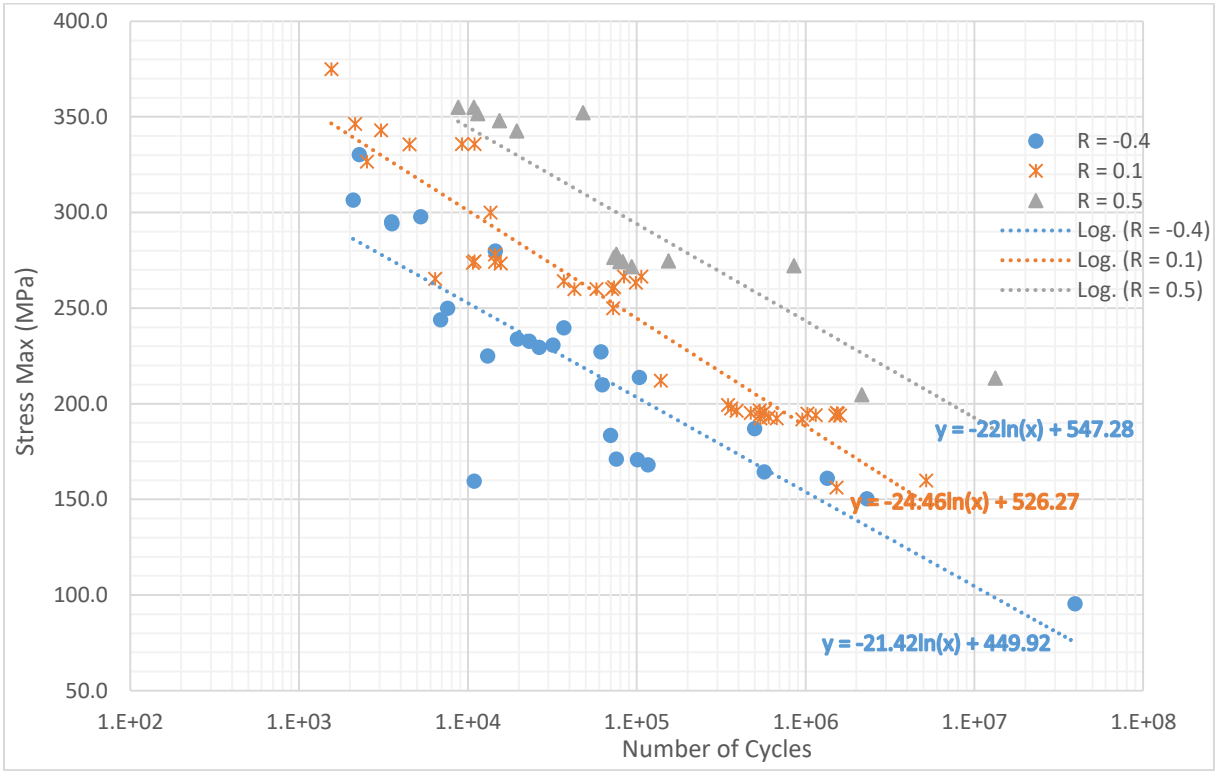

Figure 26: S-N curves for different stress ratios from Optimat project

The approach used for validation in this case is to extrapolate the results for a particular stress ratio using the experimental data from the other two stress ratios. For example, the extrapolated data points for *R = 0.1* would correspond to those extrapolated from experimental data points of *R = -0.4* and *R = 0.5*.

The linear extrapolation technique using the Goodman diagram, when results for a single *R* ratio are available, is used to predict the data. The three stress ratios chosen are all for tensile dominated fatigue. *R=-0.4* corresponds to an alternating stress cycle, but the magnitude of the tensile stress is

more than the compressive, and hence the former is expected to dictate the fatigue failure. Hence, Equation 9, which extrapolates between the Goodman diagram data point for available *R* ratio and the data point for ultimate tensile static failure, is used for the extrapolation.

5.3.2 Results and Discussion

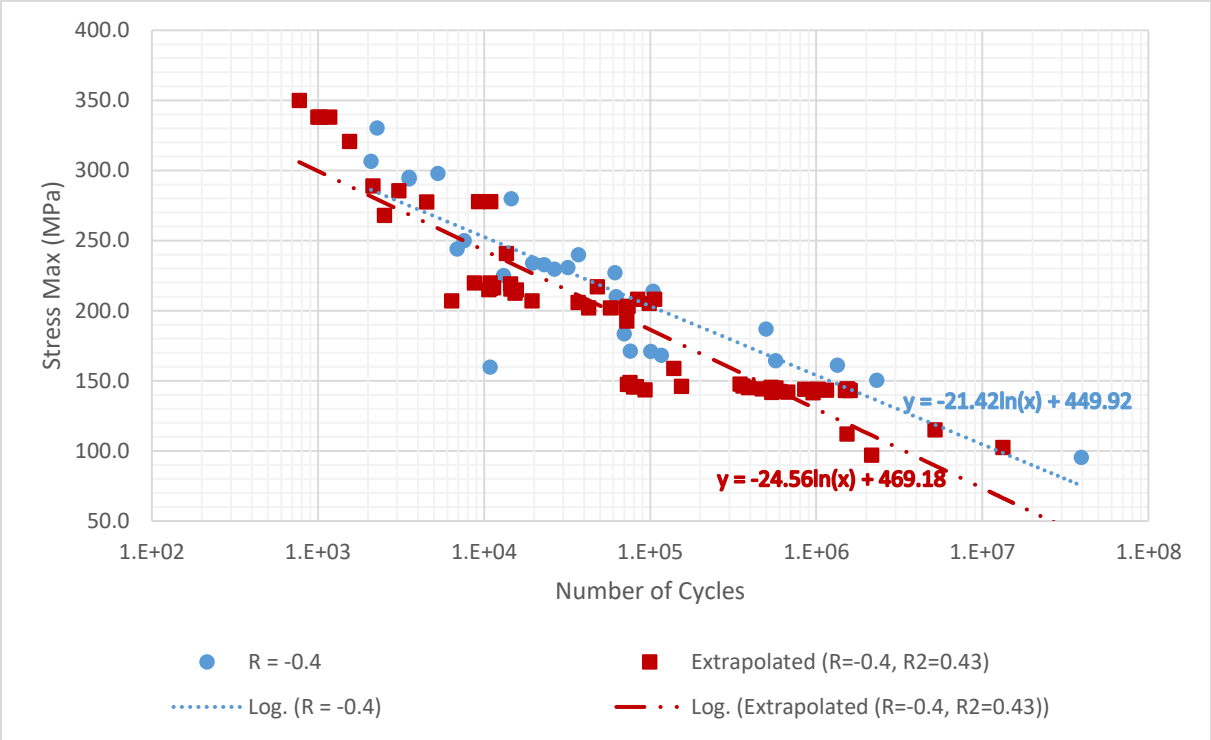

Figure 27: Experimental vs Extrapolated S-N curve for R = -0.4

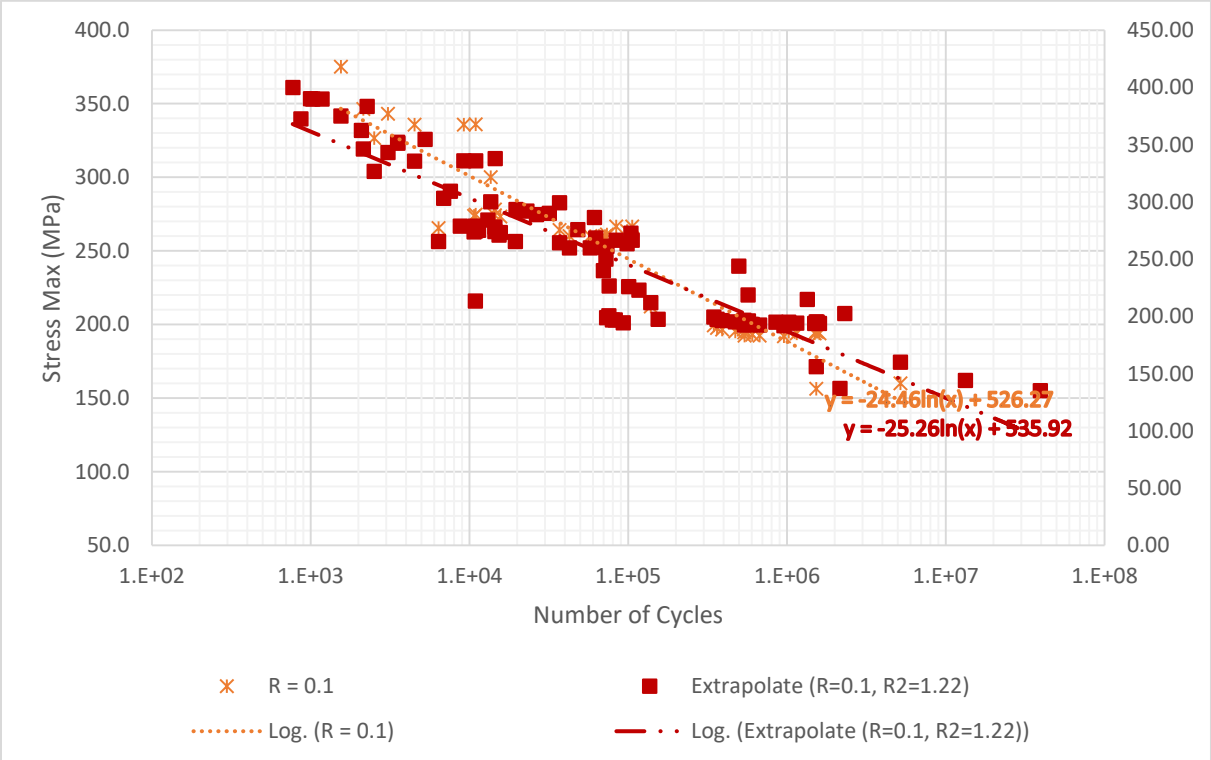

Figure 28: Experimental vs Extrapolated S-N curve for R = 0.1

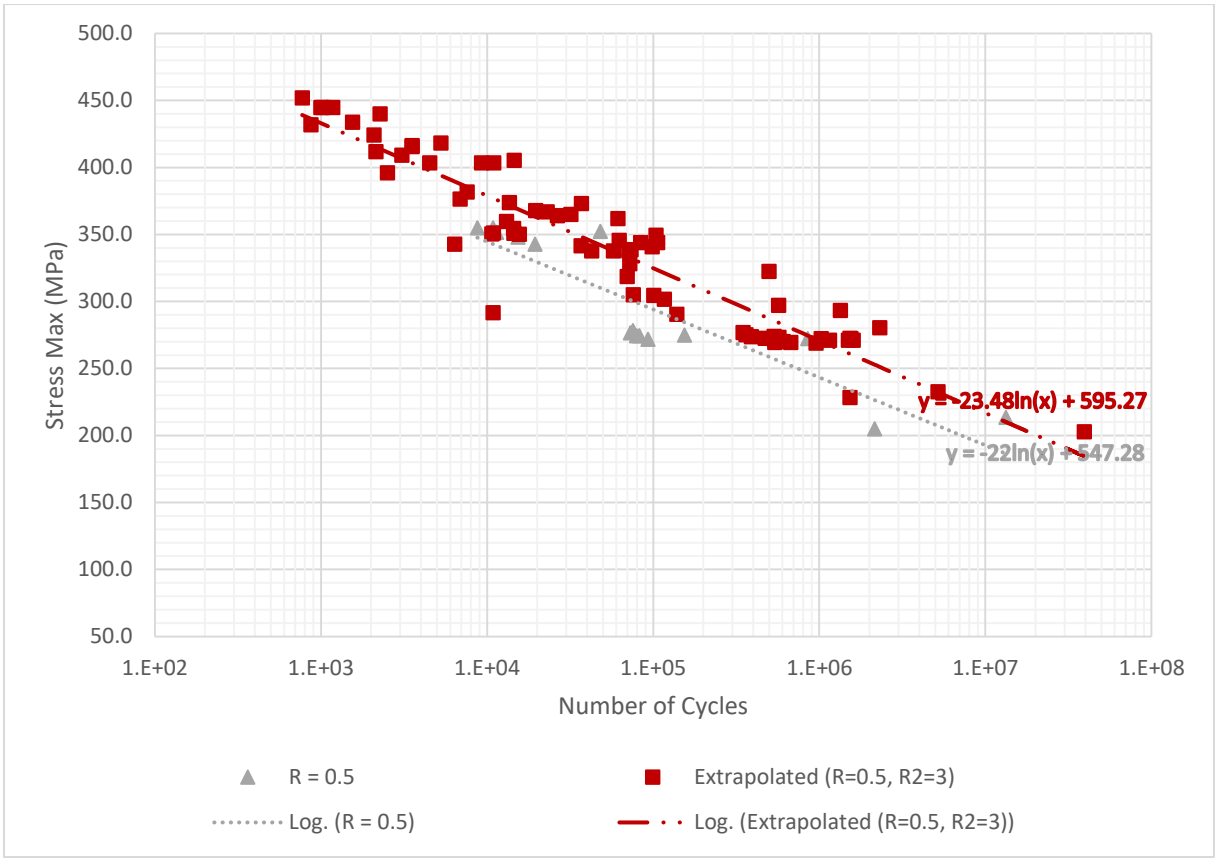

Figure 29: Experimental vs Extrapolated S-N curve for R = 0.5

Figure 27, Figure 28, and Figure 29 show the comparison between the S-N curve experimental data available from the Optimat database, and the extrapolated S-N curve using the linear extrapolation method for *R* ratios -0.4, 0.1 and 0.5 respectively. The red square blocks represent the extrapolated data points for each case.

As can be seen visually, there is a good correlation between the extrapolated data points and those obtained experimentally. For the tensile-tensile fatigue cases (*R=0.1* and *R=0.5*), there is a maximum discrepancy of 6.7% in the slope of the S-N curve. For the alternating fatigue case, a discrepancy of 14% is observed in the slope of the S-N curve; however, this discrepancy is mainly observed at lower stress intensities closer to the fatigue threshold.

It may be remarked that this validation is only performed for tensile dominated fatigue. The Optimat database did not have sufficient data points to perform a comparative validation for the compression dominated fatigue tests. In general, the compression tests are more difficult to perform, due to the complexity in the test fixture, and the choice of a suitable test specimen. The failure mechanisms involved in compression based fatigue are also diverse, leading to a need for more rigorous validation case studies.

As a preliminary step in the validation process, the linear extrapolation technique seems to provide promising results. However, it needs to be verified for compressive fatigue applications. The ease of carrying out the extrapolation needs to be highlighted, when compared with the extensive effort needed to experimentally obtain the S-N curve for a new stress ratio. As the method uses a simple algebraic expression to account for the effect of stress ratio, it is a promising technique that can be included in the global fatigue analysis methodology.

6 DISCUSSIONS AND CONCLUSION

The intricacy of characterizing, predicting and analysing fatigue of composite tidal turbine blades was highlighted through an extensive literature review. The complexity of the design problem impedes the development of a global fatigue analysis methodology that encompasses all its nuances; and the absence of such a global framework in the existing literature is notable. The primary objective of this task of the RealTide project was to address this knowledge gap, and contribute to defining a global fatigue analysis methodology for tidal turbine blade design applications.

From a structural design perspective, it is of paramount importance to take into account the fatigue behaviour of the blades. Fatigue, being a dynamic and long-term phenomenon, is computationally cost intensive. Existing industry practice, even for isotropic metallic materials, is to use fatigue life models to predict the fatigue behaviour. In composite applications, the uncertainty in the material behaviour can lead to very high design safety factors, as was elucidated in Table 1 in Section 2.4. The development of the global fatigue analysis methodology would be an important step towards reducing these safety factors, reducing the extent of over-design of blade scantling.

The global fatigue analysis methodology has been embedded with sub-scale methodologies, which are based on the micro-mechanical behaviour of composite laminates. A significant focus shift has been proposed, by moving away from the classical approach of characterising the fatigue behaviour of the entire laminate, towards an approach that leans towards the fatigue behaviour at the ply scale and the micro-mechanics (fibre/matrix) scale. Such approaches are expected to have wider utility for future fatigue analysis of composite laminates in multiple and diverse applications.

The experimental campaign was aimed at providing a link between the proposed theoretical models and their practical applications. Fatigue characterisation, requiring a time-intensive testing campaign, it was not practically possible to validate all the proposed methodologies. The tests were performed for laminate stacking sequences that are typically used in tidal turbine blades, and hence shed light on their expected fatigue behaviour. Validation case studies have been performed with the available test results. However, these are only for limited cases; and further testing campaigns are required to complete the validation and suitability of all the proposed methodologies. Important effects such as ageing, and ply delamination are yet to be included in the proposed methodology; experimental campaigns focused on these aspects would push forward such an implementation. The validation of the global fatigue analysis methodology is still a long way ahead; however, the results from the full scale blade testing under Task 4.4 of the RealTide project should be an important starting point towards determining the suitability of the proposed global methodology, in validating quasi-static design assumptions.

The outcome at the end of Task 1.4 of the RealTide project is that a framework has been laid which will lead to better understanding of the fatigue behaviour of composite laminates in the application of tidal turbine blades. A guidance framework for identifying the sources of fatigue loads in a tidal turbine operating environment was proposed in Section 3.4, thereby leading to a procedure that generates a realistic long-term fatigue load distribution. In addition, the ply-by-ply and micro-mechanical fatigue models proposed can have broader applications for composite laminates in general. Many of the formulations have been developed with appropriate simplifications and assumptions in order to have an applicable methodology for designers. The global framework is well adapted to assimilate any improved models for fine-tuning the predictive capability and improving current limitations.